NASA-TP-1554 19800004880

NASA Technical Paper 1554

Two-Impulse Reorientation of Asymmetric Spacecraft

C. William Martz

DECEMBER 1979

NASA

NASA Technical Paper 1554

Two-Impulse Reorientation of Asymmetric Spacecraft

C. William Martz
Langley Research Center
Hampton, Virginia

National Aeronautics
and Space Administration

**Scientific and Technical
Information Branch**

1979

SUMMARY

An investigation has been conducted to determine minimum "maneuver costs" for attitude reorientation of spacecraft of all possible inertial distribution over a wide range of maneuver angles by use of a two-impulse coning method of reorientation. Maneuver cost is proportional to the product of fuel consumed (total impulse) and time expended during a maneuver. Assumptions included external impulsive control torques, rigid-body spacecraft rest-to-rest maneuvers, and no disturbance torques.

Results are presented in terms of average cost and standard deviation for various maneuver ranges. Costs of individual reorientations can be calculated with the computer program included.

INTRODUCTION

Two-impulse attitude reorientation is a method of reorientation in which torque impulses are used to initiate and (later) to terminate free precessional and nutational motion of a body. Between torque impulses, the spinning body coasts undisturbed through some desired attitude change. The method has potential application to maneuvering spacecraft capable of producing directed external torque impulses.

Attitude reorientation by means of torque impulses has been investigated by several authors (refs. 1 to 4). Reference 1 presents a two-impulse reorientation scheme for large-angle spin-axis reorientations of spinning axisymmetric bodies. Spin-axis or pointing-axis reorientations are defined as general reorientations with final attitude being arbitrary about the spin or pointing axis. Reference 2 extends the spin-axis reorientations of reference 1 to asymmetric bodies. However, precession angle is restricted to 180° and spin-axis inertia must be larger than inertias about transverse axes. Reference 3 introduces a statistical "average cost" for general reorientations of nonspinning bodies over a specified maneuver-angle range and compares two-impulse reorientation costs with costs of other maneuver schemes. Results are limited, however, to elongated axisymmetric bodies. Reference 4 extends previous results to include two-impulse general reorientation costs for nonspinning axisymmetric foreshortened bodies. Also, two-impulse reorientation costs are obtained for pointing-axis reorientations of asymmetric nonspinning bodies of all possible inertial distribution. Finally, reference 4 presents three-impulse general reorientation costs for asymmetric nonspinning bodies. These maneuvers consisted of a basic precessional-nutational motion followed by an impulsive spin maneuver. This motion combination was required to satisfy an arbitrary constraint that initial and final angles between the spin axis and momentum vector be equal.

The present paper also presents general reorientation costs for nonspinning asymmetric bodies. However, the aforementioned motion constraint was eliminated

through the use of elliptic functions and a computational scheme involving nested Newton-Raphson iterative loops. As a result, general two-impulse solutions involving precessional-nutational motion were found with significantly reduced costs.

In the present investigation, reaction thrusters are assumed to initiate and terminate all maneuvers with impulsive torques of negligible duration. Other assumptions include rigid-body spacecraft, lack of disturbance torques, and zero initial and final attitude rates.

The product of total maneuver impulse (proportional to fuel consumed) and total maneuver time is determined for the various solution paths available for each maneuver. This product is then nondimensionalized by spacecraft inertia about the intermediate axis and is referred to as the cost function for that maneuver. Since total impulse and maneuver time are inversely proportional for impulsive maneuvers, results are independent of each of these quantities. The desired or optimal solution is defined as the solution associated with the smallest cost function for each maneuver.

Since it was assumed that all reorientations within a given range of maneuver angle are equally probable, optimal costs for a large number of statistically representative reorientations within a given maneuver range were averaged to represent reorientation costs for that maneuver range. Maneuver ranges of $\pi/360$, $\pi/4$, $\pi/2$, $3\pi/4$, and π radians were used. These results are intended primarily for reorientation cost comparisons of the two-impulse coning method with other reorientation methods. However, such comparisons are not included in the present paper.

Although costs for individual reorientations are not presented, such costs can be determined, if necessary, through the use of the computer program presented in appendix A.

SYMBOLS

$cn(u,m)$ $dn(u,m)$ $sn(u,m)$	Jacobian elliptic functions (see eqs. (12))
F	nondimensional asymmetry factor defined by equation (9b)
H	total angular momentum
H_x, H_y, H_z	angular momentum components along x-,y-,z-axes, respectively
H_{xy}	angular momentum in transverse plane, $\sqrt{H_x^2 + H_y^2}$
I_x, I_y, I_z	principal body inertias about x-,y-,z-axes, respectively; I_y is intermediate moment of inertia
m	parameter of Jacobian elliptic functions defined in equation (14e)

P,Q,R	motion constants (see eqs. (14a) to (14c))
P_x	inertial factor (see eq. (27))
Q_2	cost function (see eq. (26))
$Q_{2,A},Q_{2,T}$	axial and transverse components of Q_2, respectively (see eqs. (25))
$Q_{2,sw}$	product of total impulse and total time divided by I_y for coning maneuver where thrusters on spin axis can be swiveled
R_1,R_2,R_3	sequential Euler angle rotations about z-,y-,z-axes, respectively, relating body axes before and after reorientation (see fig. 4); R_2 is also referred to as maneuver angle
$R_{2,max}$	maneuver range, rad ($0 \leq R_2 \leq R_{2,max}$)
R_{2C}	maneuver angle transformed for x-axis maneuver
SDA	ratio of standard deviation to average cost
s	$= \frac{1}{2}(\theta_o + R_2 + \theta_f)$
T	kinetic energy (see eqs. (15))
t	time, sec
u	argument of elliptic function defined in equation (13)
X,Y,Z	inertial coordinate axis system
x,y,z	body principal coordinate axis system; unless otherwise specified, z is spin axis
x'_f	x_f-axis translated from mass center along z_f-axis
x'_o	x_o-axis translated from mass center along z_o-axis
λ	constant of linearity (see eqs. (13) and (14d))
Φ	initial base angle of spherical triangle, used to start iterative solutions, $\pi - R_1 - \phi_o$
ψ,θ,ϕ	rotation sequence of Euler angles about z-,y-,z-axes, respectively, relating inertial and body coordinate axis systems
$\dot{\psi},\dot{\theta},\dot{\phi}$	precession rate, nutation rate, and spin rate, respectively; referred to as Euler rates
$\omega_x,\omega_y,\omega_z$	body rates about x-,y-,z-axes, respectively

Subscripts:

av	average value (with respect to time) during maneuver
f	value at finish of coning maneuver
max	maximum value
new	value from present iteration
o	value at start of coning maneuver
old	value from previous iteration
start	value to start iterative solution

ANALYSIS

Equations of Motion

Two reference frames used in the analysis of the impulse coning method of attitude reorientation are illustrated in figure 1. The body principal axis system x,y,z is related to an inertial axis system X,Y,Z by an Euler rotation sequence ψ,θ,ϕ about body axes z,y,z, respectively. Note that ψ and Z are chosen to be in the same direction as the total angular momentum H. Angular momentum H is established for each reorientation maneuver by the initial torque impulse of the thrusters. Reaction thrusters are assumed to be fixed along the x,y,z body axes to produce torques about the y-,z-,x-axes, respectively. Without loss of generality, θ is restricted to $0 < \theta < \pi/2$.

The relationships between inertial rates and body rates ω_x, ω_y, and ω_z, as determined from figure 1(a), are

$$\left.\begin{aligned} \dot{\psi} &= \frac{\omega_y \sin\phi - \omega_x \cos\phi}{\sin\theta} \\ \dot{\theta} &= \omega_y \cos\phi + \omega_x \sin\phi \\ \dot{\phi} &= \omega_z - \dot{\psi}\cos\theta \end{aligned}\right\} \tag{1}$$

The angular momenta along the body axes (from fig. 1(b)) are

$$H \cos\theta = I_z\omega_z \tag{2a}$$

$$H \sin\theta \sin\phi = I_y\omega_y \tag{2b}$$

$$-H \sin\theta \cos\phi = I_x \omega_x \tag{2c}$$

Combining equations (1) and (2) yields the Euler rate equations governing the coning motion, which are

$$\left.\begin{aligned} \dot{\psi} &= H\left(\frac{\sin^2\phi}{I_y} + \frac{\cos^2\phi}{I_x}\right) \\ \dot{\theta} &= H\left(\frac{1}{I_y} - \frac{1}{I_x}\right)\sin\theta \sin\phi \cos\phi \\ \dot{\phi} &= H\frac{\cos\theta}{I_z} - \dot{\psi}\cos\theta \end{aligned}\right\} \tag{3}$$

A two-impulse coning maneuver is performed as follows: The body, initially at rest in inertial space, is acted upon by an external-control-torque impulse of negligible duration with predetermined components along the x-, y-, and z-axes. This causes the body to spin about its z-axis and precess about the Z-axis with nutational motion. After a given time during which the body freely rotates to the desired inertial attitude, a second control impulse terminates all motion.

Figure 2 illustrates the maneuver geometry and shows the axial and transverse momentum components labeled $H_{z,o}$ and $H_{xy,o}$ generated by the initial impulse. Also, the momentum components which terminate the motion are shown as $H_{z,f}$ and $H_{xy,f}$. The initial body-axis system x_o, y_o, z_o is included to illustrate the orientation of H in body coordinates.

Candidate coning solutions to equation (3) must include maneuvers with negative precession rates ($\dot{\psi} < 0$) as well as maneuvers with positive precession rates. Also, solution paths can be classified as long or short, depending upon whether the total change in precession angle is more or less than π radians. Four alternative solution paths (nutational motion suppressed) are illustrated in figure 3 for a reorientation example.

The spherical geometry of a generalized reorientation maneuver R_1, R_2, R_3 is shown in figure 4. By definition, a R_1, R_2, R_3 maneuver is any specified set of sequential Euler angle rotations about the z,y,z body axes, respectively, which reorient the body from its initial attitude to some final desired attitude.

Parameter relationships for the coning motion were determined from the geometry of figure 4. For the spherical triangle with sides θ_o, R_2, and θ_f, reference 5 specifies the following relationships:

Napier's analogies

$$\tan\left\{\frac{1}{2}\left[\psi_f - (\phi_f - R_3)\right]\right\} = \frac{\sin\left[\frac{1}{2}(R_2 - \theta_o)\right]}{\sin\left[\frac{1}{2}(R_2 + \theta_o)\right]} \cot\left[\frac{1}{2}(\pi - \phi_o - R_1)\right] \tag{4a}$$

$$\tan\left\{\frac{1}{2}\left[\psi_f + (\phi_f - R_3)\right]\right\} = \frac{\cos\left[\frac{1}{2}(R_2 - \theta_o)\right]}{\cos\left[\frac{1}{2}(R_2 + \theta_o)\right]} \cot\left[\frac{1}{2}(\pi - \phi_o - R_1)\right] \tag{4b}$$

Half-angle formula

$$\tan\left[\frac{1}{2}(\pi - \phi_o - R_1)\right] = \frac{\sqrt{\sin(s - \theta_o)\sin(s - R_2)\sin(s - \theta_f)/\sin(s)}}{\sin(s - \theta_f)} \tag{5}$$

where

$$s = \frac{1}{2}(\theta_o + R_2 + \theta_f)$$

Law of sines

$$\frac{\sin\theta_f}{\sin(\pi - \phi_o - R_1)} = \frac{\sin\theta_o}{\sin(\phi_f - R_3)} = \frac{\sin R_2}{\sin\psi_f} \tag{6}$$

Gauss's formula

$$\cos\left[\frac{1}{2}(\pi - \phi_o - R_1)\right] = \frac{\cos(\theta_f/2)\,\sin\left[\frac{1}{2}(\psi_f + \phi_f - R_3)\right]}{\cos\left[\frac{1}{2}(R_2 - \theta_o)\right]} \tag{7}$$

Equations (6) and (7) were used only to check solutions.

In addition to the geometric relationships, certain dynamic constraints were utilized. For example, the time between initial and final impulse (maneuver time or precession time) can be expressed by

$$t_f - t_o = \frac{\psi_f - \psi_o}{\dot{\psi}_{av}} \tag{8}$$

where ψ_o and t_o are set equal to zero by choice and $\dot{\psi}_{av}$ is determined by integrating the first of equations (3) to obtain

$$\dot{\psi}_{av} = H\left(\frac{\cos^2\phi}{I_x} + \frac{\sin^2\phi}{I_y}\right)_{av} \approx \frac{H}{\phi_f - \phi_o}\int_{\phi_o}^{\phi_f}\left(\frac{\cos^2\phi}{I_x} + \frac{\sin^2\phi}{I_y}\right)d\phi$$

or

$$\dot{\psi}_{av} \approx \frac{H}{I_x}(F) \tag{9a}$$

where

$$F = \frac{I_x + I_y}{2I_y} + \frac{I_y - I_x}{2I_y}\,\frac{\sin(2\phi_f) - \sin(2\phi_o)}{2(\phi_f - \phi_o)} \tag{9b}$$

Equation (9a) represents the average $\dot{\psi}$ with respect to ϕ over the coning maneuver and, thus, is an approximation to the average ψ with respect to time required in equation (8). However, the error of this approximation was found to be small (about 1/2 percent on the average). Combining equations (8) and (9) gives

$$\psi_f \approx \frac{Ht_f F}{I_x} \tag{10}$$

Another dynamic constraint to the motion, derived in reference 4, defines the maximum half-cone angle θ_{max} in terms of the inertias and Euler angles θ and ϕ. For polhodes about the z-axis,

$$\theta_{max} = \tan^{-1}\left[\sqrt{\frac{I_y(I_z - I_x) + I_x(I_z - I_y)\tan^2\phi}{I_z(I_x - I_y) + I_x(I_z - I_y)/(\tan^2\theta\cos^2\phi)}}\right] \tag{11a}$$

and for polhodes about the x-axis,

$$\theta_{max} = \tan^{-1}\left[\sqrt{\frac{I_y(I_x - I_z) + I_z(I_x - I_y)\tan^2\phi}{I_x(I_z - I_y) + I_z(I_x - I_y)/(\tan^2\theta\cos^2\phi)}}\right] \tag{11b}$$

The term "polhode" is discussed in appendix B. Equations (11) derive from the fact that energy and momentum of the body remain constant throughout the motion. These equations were used not only to insure that tentative θ,ϕ combinations produced real values for θ_{max} but also to relate dynamically the initial and final θ,ϕ combinations through a constant θ_{max}.

Returning now to equation (3), it is noted that the Euler rate equations are nonlinear and have no known analytical solution involving only elementary functions. However, reference 6 formulates these equations (with the ψ and ϕ symbols interchanged) along with a solution in terms of Jacobian elliptic functions. The required functional relationships are

$$sn(u,m) = \frac{\sin\theta\sin\phi}{Q} \tag{12a}$$

$$cn(u,m) = \frac{\sin\theta\cos\phi}{P} \tag{12b}$$

$$dn(u,m) = \frac{\cos\theta}{R} \tag{12c}$$

where u is the linear function of time

$$u = u_o + \lambda t \tag{13}$$

and the constants P, Q, R, λ, and the parameter m can be written as

$$P = \sqrt{\frac{I_x\left[1 - (2TI_z/H^2)\right]}{I_x - I_z}} \tag{14a}$$

$$Q = \sqrt{\frac{I_y\left[1 - (2TI_z/H^2)\right]}{I_y - I_z}} \tag{14b}$$

$$R = \sqrt{\frac{I_z\left[(2TI_x/H^2) - 1\right]}{I_x - I_z}} \tag{14c}$$

$$\lambda = H\sqrt{\frac{(I_y - I_z)\left[(2TI_x/H^2) - 1\right]}{I_xI_yI_z}} \tag{14d}$$

$$m = \frac{(I_x - I_y)\left[1 - (2TI_z/H^2)\right]}{(I_y - I_z)\left[(2TI_x/H^2) - 1\right]} = (\text{Modulus})^2 \tag{14e}$$

The energy T and angular momentum constants of the motion are given by

$$\left.\begin{aligned} T &= \frac{1}{2}(I_x\omega_x^2 + I_y\omega_y^2 + I_z\omega_z^2) \\ H^2 &= (I_x\omega_x)^2 + (I_y\omega_y)^2 + (I_z\omega_z)^2 \end{aligned}\right\} \tag{15}$$

and the motion constant $2T/H^2$ which occurs in equations (14) can be expressed through equations (2) and (15) as

$$\frac{2T}{H^2} = \sin^2\theta\left(\frac{\cos^2\phi}{I_x} + \frac{\sin^2\phi}{I_y}\right) + \frac{\cos^2\theta}{I_z} \tag{16}$$

It can be seen from equations (2) and (12) that the body rate solutions are directly related to these Jacobian elliptic functions as follows:

$$\left.\begin{aligned} \omega_x &= -HP\ cn(u,m)/I_x \\ \omega_y &= HQ\ sn(u,m)/I_y \\ \omega_z &= HR\ dn(u,m)/I_z \end{aligned}\right\} \tag{17}$$

Also from equations (12),

$$\theta = \cos^{-1}\left[R\ dn(u,m)\right] \tag{18}$$

and

$$\phi = \tan^{-1}\left[\frac{Q\ sn(u,m)}{P\ cn(u,m)}\right] \tag{19}$$

Equations (12) to (19) were not used to generate time histories of body rates or Euler angles, but rather served to derive Ht_f for equation (10).

Equation (13) was evaluated at t_f and combined with equation (14d) to yield

$$Ht_f = \frac{u_f - u_o}{\sqrt{\dfrac{(I_y - I_z)\left[(2TI_x/H^2) - 1\right]}{I_xI_yI_z}}} \tag{20}$$

Here, the quantity u_o was calculated by means of the arithmetic-geometric mean process and successive use of the descending Landen transformation (both discussed in reference 7) from $sn(u_o,m)$ which in turn was determined from the first of equations (12) evaluated at t_o. The value of u_f was determined similarly from $sn(u_f,m)$ which was obtained from the first of equations (12) evaluated at t_f. Finally, equations (10) and (20) are combined to generate the dynamic expression for ψ_f:

$$\psi_f = \frac{(u_f - u_o)F/I_x}{\sqrt{\frac{(I_y - I_z)\left[(I_x 2T/H^2) - 1\right]}{I_x I_y I_z}}} \tag{21}$$

Solution of Equations

Equations (4a), (4b), (11a) or (11b), and (5) which govern variables ψ_f, ϕ_f, θ_f, and ϕ_o, respectively, were solved in a Newton-Raphson iterative (inner) loop in the order specified for a given value of θ_o. Starting and stopping conditions are given subsequently. This result was then used in a second Newton-Raphson iterative (outer) loop involving the dynamic value of ψ_f (from eq. (21)) and the relationship

$$\theta_{o,new} = \theta_{o,old}\left(\left|\frac{\psi_f}{\psi_f \text{ dynamic}}\right|\right)^{0.1} \tag{22}$$

The inner loop equations were then solved again (by iteration) for the new value of θ_o from equation (22). This process continued with inner loop convergence for successive "new" values of θ_o until the outer loop converged and all equations were satisfied simultaneously. The convergence condition for the inner loop was that input and output values of θ_o be equal within ±0.0001 percent. For the outer loop, convergence was defined as input and output values of θ_o being equal within ±0.01 percent.

The values of θ_o and ϕ_o used to start the iterative process were determined from

$$\phi_{o,start} = \pi - R_1 - \Phi \tag{23a}$$

$$\theta_{o,start} = \tan^{-1}\left[\frac{\tan (R_2/2)}{\cos \Phi}\right] \tag{23b}$$

Equation (23a) is an expression for the initial base angle Φ of the spherical triangle (see fig. 4), and equation (23b) is a geometric relationship for a spherical triangle initially assumed to be equilateral.

Solutions were attempted for 16 separate values of Φ (spread over the range $0 < \Phi < \pi/2$) for each solution path. Possible solution paths (for each given maneuver and inertial distribution) included all eight combinations of long and short paths, positive and negative precession rates, and polhodes about the x- and z- axes. All such solutions were determined if possible and

the one associated with minimum maneuver costs was retained for computing the "average cost" of reorientations presented for each maneuver range. The listing and documentation of computer program IMP2, used to determine these solutions, is presented in appendix A.

REORIENTATION COSTS

General Considerations

As mentioned in the "Introduction," a cost function equal to the product of total maneuver impulse (proportional to fuel consumed) and total maneuver time (nondimensionalized by spacecraft inertia about the intermediate principal axis) is determined for the various solution paths available for each maneuver. The desired or optimum path is defined as the path associated with the smallest cost function for each coning maneuver. Since total impulse and maneuver time are inversely proportional for impulsive maneuvers, results are independent of each of these quantities.

It is assumed that all reorientations within a given maneuver range $R_{2,max}$ are equally probable. Therefore, reorientation costs were sampled within each given maneuver range by systematically computing optimum costs for combinations of R_1, R_2, and R_3 at equally spaced intervals throughout the sample space limits $-\pi \leq R_1 \leq \pi$, $0 \leq R_2 \leq R_{2,max}$, and $-\pi \leq R_3 \leq \pi$ where $R_{2,max} = \pi/360$, $\pi/4$, $\pi/2$, $3\pi/4$, and π radians. These optimum-cost functions were then weighted (according to likelihood of occurrence) and averaged as follows:

$$(\text{Average cost}) = \frac{\sum \left[(\text{Optimum cost}) \times \sin R_2\right]}{\sum (\sin R_2)}$$

In addition, the standard deviation of the optimum-cost functions was determined with the relationship

$$(\text{Standard deviation}) = \sqrt{\frac{\sum \left[(\text{Optimum cost})^2 \times \sin R_2\right]}{\sum (\sin R_2)} - (\text{Average cost})^2}$$

Cost Equations

The impulse (and thus momentum) required to initiate and terminate coning maneuvers has transverse components

$$H_{xy,o} = H \sin \theta_o \qquad H_{xy,f} = H \sin \theta_f$$

and axial components

$$H_{z,o} = H \cos \theta_o \qquad H_{z,f} = H \cos \theta_f$$

as shown in figure 2.

For reaction thrusters fixed along the x, y, and z body axes to produce torques about the y-, z-, and x-axes, respectively, the cost function $[(\text{Total impulse}) \times (\text{Total time})]/I_y$ for the two-impulse coning maneuver is

$$Q_2 = Q_{2,A} + Q_{2,T} \tag{24}$$

where the axial and transverse components are, respectively,

$$\left.\begin{aligned} Q_{2,A} &= \frac{|H|t_f}{I_y}(\cos \theta_o + \cos \theta_f) \\ Q_{2,T} &= \frac{|H|t_f}{I_y}\left[\sin \theta_o \left(|\sin \phi_o| + |\cos \phi_o|\right) + \sin \theta_f \left(|\sin \phi_f| + |\cos \phi_f|\right)\right] \end{aligned}\right\} \tag{25}$$

By combining equations (10), (24), and (25), the cost function can also be expressed as

$$Q_2 = \frac{I_x|\psi_f|}{I_y F}\left[\sin \theta_o \left(|\sin \phi_o| + |\cos \phi_o|\right) + \sin \theta_f \left(|\sin \phi_f| + |\cos \phi_f|\right) + \cos \theta_o + \cos \theta_f\right] \tag{26}$$

If the thruster pair fixed on the spin axis to produce torques about the x-axis is allowed to swivel about the spin axis, the components of $Q_{2,T}$ can be minimized (reduced about 21 percent on the average) at the expense of a relatively small thruster prepositioning term Q_p with the result expressed as

$$Q_{2,sw} = \frac{|H|t_f}{I_y}(\sin \theta_o + \cos \theta_o + \sin \theta_f + \cos \theta_f) + Q_p$$

RESULTS AND DISCUSSION

The results of this investigation are primarily the costs of attitude reorientation by the two-impulse coning method. These are presented in the form of average cost (over a given maneuver range) as functions of $1 - (I_z/I_y)$, I_x/I_y, and $R_{2,max}$ for bodies of all possible inertial distribution which are identified in reference 4 and presented in figure 5. Although costs for the thousands of required individual reorientations could not be presented, such costs can be calculated, if desired, by means of the computer program presented in appendix A.

Each of the hundreds of two-impulse maneuver solutions used to generate average costs for individual inertial configurations was first determined and then independently checked by numerical integration of the motion equations to assure that the desired maneuver was accomplished within an acceptable tolerance. In this respect, maximum errors in ψ_f, proportional to $R_{2,max}$, were found to be about ±0.5 percent on the average. Corresponding errors in θ_f and ϕ_f were less than ±0.005 percent. Two-impulse coning solutions for general reorientations of asymmetric bodies were anticipated in reference 4 on the basis that the three input quantities of the maneuver (coordinate-axis torques) should allow control of three output quantities (final Euler angles) regardless of inertial configuration. This is confirmed by the results of the present investigation. Figure 6 shows the effect of inertia distribution on average cost of reorientation for maneuver ranges of $\pi/360$, $\pi/4$, $\pi/2$, $3\pi/4$, and π radians. The curve labeled $I_x/I_y \equiv 1$ on each plot represents the family of axisymmetric bodies. Most of these results were reported in reference 4 and are included here for comparison with the asymmetric results of the present investigation which are the remaining curves of figure 6.

The axisymmetric results indicate an almost linear reduction in reorientation costs as bodies become more elongated. This is true for all maneuver ranges. Reorientation costs are also seen to be proportional to maneuver range for axisymmetric inertial configurations.

Inspection of all the results of figure 6 shows that introducing inertial asymmetries to axisymmetric bodies causes the average cost of reorientation to decrease significantly for relatively "thick" bodies. (See left side of fig. 6.) Conversely, for relatively "slender" bodies, introducing inertial asymmetry results in somewhat larger reorientation costs. In retrospect, this result could have been anticipated because x-axis inertia is the only difference between comparable asymmetric and axisymmetric bodies. Since average cost is proportional to the effective transverse inertia of a body (a value between I_x and I_y), the increase in I_x required to change the "slender" bodies from axisymmetric to asymmetric resulted in higher costs. Similarly, the decrease in I_x required to change the "thick" bodies caused a reduction in average cost.

The results of appendix C also are illustrated in figure 6. Reorientation costs for rod-shaped bodies with axial symmetry along the z-axis as well as costs for rod-shaped bodies with axial symmetry along the x-axis are in good agreement with both the axisymmetric and asymmetric results previously discussed.

Figure 7 was prepared to illustrate the effect of $R_{2,max}$ on average cost for asymmetric bodies. These curves are restricted to $I_x/I_y = 1.2$ but should be representative of other ratios. As would be expected, average cost is seen to increase with maneuver range.

The average-cost results presented in figure 6 for asymmetric bodies represent minimum-cost reorientations involving a mixture of polhodes about the x- and z-axes. Although polhode axis for minimum maneuver cost is unpredictable for individual reorientations, the polhode axis, on the average, seems to be the principal axis about which inertia is most unlike (greatest percentage difference) the y-axis (intermediate) inertia. More specifically, an inertial factor P_x for estimating the probability of polhode about the x-axis has been found empirically for $R_{2,max} = \pi$ radians to be

$$P_x = \frac{R_{x/y} - 1}{R_{x/y} - 1 + R_{y/z} - 1} \tag{27}$$

where

$R_{x/y} = I_x/I_y$ or I_y/I_x (Whichever is greater)

$R_{y/z} = I_y/I_z$ or I_z/I_y (Whichever is greater)

It follows that the inertial factor P_z for estimating the probability of polhode about the z-axis is $P_z = 1 - P_x$. Figure 8 illustrates the correlation of P_x with measured values for all results of figure 6(e).

In reference 4, reorientation by means of impulse coning was solved under the constraint that the initial and final angles between spin axis and the momentum vector be equal. This resulted in solutions involving a two-impulse coning maneuver followed by a spin-correction maneuver. As a result, costs were considerably higher than those of the present investigation which uses two-impulse coning maneuvers not requiring a follow-up spin maneuver.

Maneuver costs have been presented thus far in the form of average cost for specified maneuver ranges. Also important is the measure of how costs are dispersed about these average values which is given by their standard deviation. Ratios of standard deviation to average cost are computed along with the average-cost results. These values are presented in table I along with companion values of average cost.

Table I indicates that average costs have standard deviations of about 40 percent (of cost) for $R_{2,max} = \pi$ radians, increasing to about 65 percent as $R_{2,max}$ is reduced to $\pi/360$ radians. Thus, average-cost results do not apply accurately to individual reorientations, but rather to a large number of uniformly distributed reorientations.

CONCLUDING REMARKS

This report presents data figures which can be used to evaluate the costs of attitude reorientation by two-impulse coning for bodies of all possible inertial distribution and over the complete range of maneuver angle. Two-impulse coning is a method of general-attitude reorientation in which torque impulses are used to initiate and later to terminate free precessional and nutational motion of a body.

Costs are presented for selected inertia configurations in the form of average cost (and standard deviation) for a large number of uniformly distributed reorientations within a given maneuver range. These results, determined for five maneuver ranges, are intended primarily for cost comparisons of the two-impulse method with other reorientation methods (not included). Although costs for individual reorientations are not included, such costs can be determined, if necessary, through the use of an included computer program.

Results show that the two-impulse coning method is capable of producing general reorientations of asymmetric as well as axisymmetric bodies.

Results for axisymmetric bodies indicate that for all maneuver ranges reorientation costs become progressively smaller as the body is elongated. Also, reorientation costs are proportional to maneuver range.

The introduction of inertial asymmetry to axisymmetric bodies causes reorientation costs to decrease significantly for relatively "thick" bodies. For relatively "slender" bodies, however, the addition of inertial asymmetry results in somewhat larger reorientation costs. In all cases, however, costs are proportional to maneuver range.

Polhode axis for minimum maneuver costs is unpredictable for individual reorientations. However, for a maneuver range of π radians, polhode axis, on the average, seems to be the principal body axis about which inertia is most unlike the intermediate principal-axis inertia.

Langley Research Center
National Aeronautics and Space Administration
Hampton, VA 23665
October 25, 1979

APPENDIX A

PROGRAM IMP2

Computer program IMP2, used to determine minimum costs for two-impulse reorientation of asymmetric spacecraft, is presented in this appendix.

Symbols

Pertinent symbols used in program IMP2 and their definition or relationship to symbols used throughout the report are as follows:

ACOST — weighted average cost of maneuvers within given $R_{2,max}$,

$$\frac{\sum (Q_2 |\sin R_2|)}{\sum (|\sin R_2|)}$$

ANG — Φ, initial amplitude of AN1 used to start iterative solution

AN1,AN2 — base angles of spherical triangle, opposite sides θ_f and θ_o, respectively

B — indicator for positive (B = 0) and negative (B = 1) precession rates

EOH — $2T/H^2$

EPS — u_o

HOLD — solution terminated for HOLD = 1

HTF — Ht_f

LOH — λ/H

M — m

P,Q,R — P, Q, and R, respectively

PATH — indicator for short (PATH = 0) and long (PATH = 1) solution paths

PI — π

R1,R2,R3 — R_1, R_2, and R_3, respectively

R1C,R2C,R3C — maneuver about x polhode axis equivalent to R_1, R_2, and R_3 maneuver about z polhode axis; R2C = R_{2C}

R4,R5,R6 — I_x, I_y, and I_z, respectively

R7	θ_o
R8	ϕ_o
R10	θ_{max}
R13	ψ_f
R14	ϕ_f
R15	F
R19	θ_f
R20	latest iterative value for ϕ_o
R22	maneuver cost
R23	latest iterative value for AN1
R26	AN1 check value from equation (7)
R30	latest iterative value for θ_o
R34	ψ_f dynamic
R40,R41	lower and upper sample limit for R1, respectively
R42,R43	lower and upper sample limit for R2, respectively; R43 = $R_{2,max}$
R44,R45	lower and upper sample limit for R3, respectively
R54	sin R_2, weighting factor in cost calculation
S	s
TCOST	weighted sum of maneuver costs
TNO	weighted sum of maneuvers
UF	u_f
UO	u_o

APPENDIX A

Program Listing

```
      PROGRAM IMP2  (INPUT,OUTPUT,TAPE5=INPUT,TAPE6=OUTPUT)
      EXTERNAL EULER
      COMMON /EULER/C4,C5,C6,H
      COMMON B,PI,R1,R2,R3,R4,R5,R6,R7,R8,R10,R11,R12,R13,R14,R15,
     1R19,R20,R22,R23,R30,R31,R32,R33,R34,R53,AN1,AN2,FLG2,R73,S
     1,R61,HOLD,KOUNT,ADD,R123,R26,RET,ANG,HTF,R0,EOH,R34R,ACC,CTAVG
      EQUIVALENCE(IX,R4),(IY,R5),(IZ,R6)
      REAL IX,IY,IZ
      INTEGER CSAV
      INTEGER A,C,A1,CA1
      DIMENSION WK(21),Y(3)
      DATA A,C/1HA,1HC/
      PI=2.*ASIN(1.) $ CON=1. $ IY=100.
      NAMELIST/ICONE/IX,IY,IZ,CON,PTDEN,R40,R41,R42,R43,R44,R45
      PTDEN=12./PI $ CON=2. $ R40=R42=0. $ R44=-PI $ R41=R43=R45=PI
 1000 READ(5,ICONE)
      IF(EOF(5))14,15
   14 STOP
   15 CONTINUE
      R70=REP=TNO=TCOST=TC2=TCREP=R123=FLG2=0.
      ER1S=0.
      C22=1.E8 $ ISAV=NUM=0
      R0=.5 $ ACC=1.E-6 $ R34=100.
C    INITIALIZE MANEUVER
      R1=PR1=S51=R40+1./(2.*PTDEN)
      R2=PR2=R42+1./(2.*PTDEN)
      R3=PR3=S53=R44+CON/(4.*PTDEN)
      WRITE(6,ICONE)
      R54=ABS(SIN(R2)) $ GO TO 2
C    NEXT MANEUVER
    7 R3=PR3=R3+CON/PTDEN $ IF(R3.GT.R45)GO TO 25 $ GO TO 2
    8 R1=PR1=R1+1./PTDEN $ IF(R1.GT.R41)GO TO 24 $ GO TO 2
    9 R2=PR2=R2+1./PTDEN $ R54=ABS(SIN(R2)) $ IF(R2.GT.R43)GO TO 26
C   COMPUTE EULER COSINE MATRIX FOR MANEUVER R1,R2,R3 ABOUT Z Y Z AXES
    2 SR1=SIN(R1) $ SR2=SIN(R2) $ SR3=SIN(R3)
      CR1=COS(R1) $ CR2=COS(R2) $ CR3=COS(R3)
      B11=CR1*CR2*CR3-SR1*SR3 $ B12=SR1*CR2*CR3+CR1*SR3
      B13=-SR2*CR3 $ B21=-CR1*CR2*SR3-SR1*CR3
      B22=-SR1*CR2*SR3+CR1*CR3 $ B23=SR2*SR3
      B31=SR2*CR1 $ B32=SR2*SR1 $ B33=CR2
C   COMPUTE EULER ROTATIONS R1C, R2C,R3C ABOUT -X Y -X AXES
      R1C=ATAN2(B12,-B13) $ X3=-B33*SIN(R1C)-B32*COS(R1C)
      Y3=B22*COS(R1C)+B23*SIN(R1C) $ X2=B21*X3+B31*Y3 $ Y2=B11
      R2C=ATAN2(X2,Y2) $ R3C=ATAN2(X3,Y3) $ ANGO=.01 $ ALT=0.
    3 IF(REP.EQ.0.)GO TO 1 $ R1=-R1C $ R2=R2C $ R3=-R3C
C   INITIALIZE FOR NEWTON RAPHSON ITERATION METHOD
```

```
    1 ANG=ANGO $ B=1. $ IF(ISAV.GT.0 )B=0.
   12 HOLD=RET=0. $ KOUNT=0 $ R31=R32=R33=-10.
      R8=R61=PI-R1-(2.*B-1.)*(1.-2.*R123)*ANG
      R7=ATAN(SQRT(R4*(R6-R5)/(ABS(R6-R5)/(R6-R5)+R6*(R5-R4)*COS(R8)
     1*COS(R8)))) $ IF(R7.LT..4*R2)GO TO 18
      R31=ATAN(TAN(R2/2.)/COS(ANG))$IF(ALT.EQ.1.)R31=(R7+R31)/2.$R7=R31
      CALL THETA $ IF(HOLD.GT..5)GO TO 18
      R51=R30 $ R7=R32=(R7+R30)/2.
      CALL THETA $ IF(HOLD.GT..5)GO TO 18 $ R52=R30
    5 R90=(R52-R51)/(R32-R31) $ R7=(R51-R90*R31)/(1.-R90)
      R33=R7=ABS(ASIN(SIN(R7)))
      CONS=1.
   21 CALL THETA $ IF(HOLD.GT..5)GO TO 18 $ R53=R30
      R34A=ABS(R34R) $ IF(R34A.GT.PI)R34A=2.*PI-R34A
      IF(ABS((R34A-ABS(R13))/R34A).LE.100.*ACC)GO TO 6
      IF(ABS(R32-R52).GT.ABS(R33-R53))GO TO 22 $ IF(CONS.GT.10.)GO TO 22
      R33=R7=R0*R33+(1.-R0)*R32 $ CONS=CONS+1. $ GO TO 21
   22 R31=R32 $ R32=R33 $ R51=R52 $ R52=R53 $ GO TO 5
    6 R8=R20 $ R12=(R13+R14-R3)/2. $ R7=R30
C    SOLUTION GEOMETRY CHECK (GAUSS FORMULA)
      R26=COS(R19/2.)*SIN(R12)/COS(.5*(R2-R7))$ IF(ABS(R26).GT.1.)R26=1.
      R26=ACOS(COS(2.*ACOS(R26)))*ABS(R13)/R13
      IF(ABS((R23-R26)/R23).LE..001)GO TO 51 $ WRITE(6,4)R23,R26
C    COMPUTE MANEUVER COST
   51 R21=2.*R4*R5*R34/(R4+R5+(R5-R4)*(SIN(2.*R14)-SIN(2.*R20))/(2.*(R14
     1-R20)))
      R22=ABS(R21)*(SIN(R7)*(ABS(SIN(R20))+ABS(COS(R20)))+SIN(R19)*(
     1ABS(SIN(R14))+ABS(COS(R14)))+COS(R7)+COS(R19))/R5
C   POLHODE CONDITION DETERMINED
      A1=A $ IF((REP-.5).LT.0.)A1=C
      AN2=R14-R3 $ AN1=PI-R1-R8
   19 IF(ABS(AN2).LT.PI)GO TO 20 $ AN2=AN2-2.*PI*ABS(AN2)/AN2 $ GO TO 19
C    SOLUTION GEOMETRY CHECK (SIN RULE)
   20 F40=SIN(R13)/SIN(R2) $ F41=SIN(AN1)/SIN(R19) $F42=SIN(AN2)/SIN(R7)
      IF(ABS((2.*F40-F41-F42)/F40).LE..007)GO TO 52
      WRITE(6,4)F40,F41,F42
C   LOWEST COST SOLUTION IS SAVED
   52 IF(R22.GE.C22)GO TO 18
      CA1=A1 $ CAN1=AN1 $ CAN2=AN2 $ CREP=REP $ CCR1=R1 $ CCR2=R2
      CCR3=R3 $ CSAV=ISAV $ C7=R7 $ C8=R8 $ C14=R14 $ C15=R15 $ CHTF=HTF
      C34R=R34R $ C19=R19 $ C22=R22 $ C34=R34 $ CB=B $ C23=R23 $ C26=R26
      C11=R11 $ C12=R12 $ C13=R13 $ KOUNTC=KOUNT $ C123=R123 $AN=ANG
      C4=R4 $ C5=R5$ C6=R6
      STAVG=CTAVG
C    CHANGE STARTING POINT AND COMPUTE ALTERNATE SOLUTION
   18 ANG=ANG+.2 $ IF(ANG.LE.PI/2.)GO TO 12 $ NUM=NUM+1
```

```
      IF(R123.GT..5)GO TO 10 $ R123=1. $ GO TO 1
   10 R123=0. $ ISAV=ISAV+1 $ IF(ISAV.LT.2)GO TO 1 $ ISAV=0
C  SETTING CONDITIONS FOR POLHODE ABOUT(A) AXIS OR RESETTING FOR
C  POLHODE ABOUT (C) AXIS
      SR4=R4 $ R4=R6 $ R6=SR4
      IF(REP.GT..5)GO TO 11 $ REP=1. $ GO TO 3
   11 REP=0. $ R1=PR1 $ R2=PR2 $ R3=PR3
                                      IF(ALT.EQ.1.)GO TO 28
      IF(ANGO.EQ..11)GOTO23$ IF(ANGO.EQ..01)ANGO=.11$ IF(ALT.EQ.0.)GOTO1
   23 IF(ABS(C34).LE.2.*PI)GO TO 17 $ ANGO=.02 $ ALT=1. $ GO TO 1
   28 IF(ABS(C34).LE.2.*PI)GO TO 17
      IF(ANGO.EQ..17)GO TO 16 $ IF(ANGO.EQ..07)ANGO=.17
      IF(ANGO.EQ..12)ANGO=.07 $ IF(ANGO.EQ..02)ANGO=.12 $ GO TO 1
   17 IF(C22.EQ.1.E8)GO TO 7
C  COMPUTE STATISTICALLY AVERAGE MANEUVER COST
   13 TNO=TNO+R54 $ TCOST=TCOST+C22*R54 $ ACOST=TCOST/TNO
      TC2=TC2+C22*R54*C22
      TCREP=TCREP+CREP $ R70=R70+1.
C  MATRIX TRANSFORMATION CHECK FOR EACH MANEUVER
      S20=SIN(C7) $ C20=COS(C7) $ S30=SIN(C8) $ C30=COS(C8)
      S1F=SIN(C13) $ C1F=COS(C13) $ S2F=SIN(C19) $ C2F=COS(C19)
      S3F=SIN(C14) $ C3F=COS(C14) $ S1=SIN(CCR1) $ C1=COS(CCR1)
      S2=SIN(CCR2) $ C2=COS(CCR2) $ S3=SIN(CCR3) $ C3=COS(CCR3)
      MO11=C20*C30                $ MO31=-S20*C30
      M11=-S1*S3+C1*C2*C3         $ M31=-S2*C3
      MF11=-S1F*S3F+C1F*C2F*C3F   $ MF31=-S2F*C3F
      MO12=-C20*S30               $ MO32=S20*S30
      M12=-S1*C3-C1*C2*S3         $ M32=S2*S3
      MF12=-S1F*C3F-C1F*C2F*S3F   $ MF32=S2F*S3F
      MO13=S20                    $ MO33=C20
      M13=C1*S2                   $ M33=C2
      MF13=C1F*S2F                $ MF33=C2F
      MO21=S30
      M21=C1*S3+S1*C2*C3
      MF21=C1F*S3F+S1F*C2F*C3F
      MO22=C30
      M22=C1*C3-S1*C2*S3
      MF22=C1F*C3F-S1F*C2F*S3F
      M23=S1*S2
      MF23=S1F*S2F
      D11=MO11*M11+MO12*M21+MO13*M31-MF11
      D12=MO11*M12+MO12*M22+MO13*M32-MF12
      D13=MO11*M13+MO12*M23+MO13*M33-MF13
      D21=MO21*M11+MO22*M21-MF21
      D22=MO21*M12+MO22*M22-MF22
      D23=MO21*M13+MO22*M23-MF23
```

```
      D31=M031*M11+M032*M21+M033*M31-MF31
      D32=M031*M12+M032*M22+M033*M32-MF32
      D33=M031*M13+M032*M23+M033*M33-MF33
      IF(ABS(D11)+ABS(D12)+ABS(D13)+ABS(D21)+ABS(D22)+ABS(D23)+ABS(D31)
     1+ABS(D32)+ABS(D33).GT..006)
     1WRITE(6,53)D11,D12,D13,D21,D22,D23,D31,D32,D33
   53 FORMAT(1X9E11.3)
   16 CONTINUE
      WRITE(6,29)CCR1,CCR2,CCR3,C13,CHTF,C34R,C7,C19,C8,C14,CAN1,CAN2,
     1CA1,C34,C22,PR1,PR3,INT(C123),INT(C8),INT(R70),KOUNTC,AN
   29 FORMAT(1XF8.4,F7.4,F8.4,F7.3,F7.1,F7.3,2F7.4,3F8.4,F7.3,1XA1,F7.3,
     1F6.2,F6.3,F7.3,2I2,I5,I3,F5.2)
C     SOLUTION CHECK VIA NUMERICAL INTEGRATION
      N=3 $ T=0. $ H=25.*ABS(CHTF)/CHTF $ TEND=CHTF/H
      Y(1)=0. $ Y(2)=C7 $ Y(3)=C8 $ TOL=1.E-5 $ MTH=2
      GMIN=ABS(CHTF)/5.E11 $ GMAX=20. $ G=ABS(CHTF)/500.
      DO 35 I=1,900
      CALL RKF4(N,T,TEND,Y,TOL,EULER,PD,MTH,GMIN,GMAX,G,WK,IERR)
      IF(IERR.LT.0)STOP  1234 $ IF(T.GE.TEND-1.E-6)GO TO 36
   35 CONTINUE
   36 ER1=100.*ABS((Y(1)-C34)/Y(1)) $ IF(ABS(C34).GT.2.*PI)ER1=0.
      ER2=100.*ABS((Y(2)-C19)/Y(2)) $ ER3=100.*ABS((Y(3)-C14)/Y(3))
      ER1S=ER1S+ER1 $ AER1=ER1S/R70
      WRITE(6,4) Y(1),Y(2),Y(3),ER1,ER2,ER3,AER1,STAVG,C15
   27 C22=1.E8 $ GO TO 7
   25 R3=PR3=S53 $ GO TO 8
   24 R1=PR1=S51 $ SD=SQRT(TC2/TNO-ACOST*ACOST) $ SDA=SD/ACOST
      PR=TCREP/R70
      WRITE(6,4)R2,TNO,TCREP,ACOST,SD,SDA,PR,AER1
      GO TO 9
   26 SD=SQRT(TC2/TNO-ACOST*ACOST) $ SDA=ACOST/SD
      WRITE(6,4)R70,TNO,TCREP,ACOST,SD,SDA
    4 FORMAT(6X9E14.4)
      GO TO 1000 $ END


      SUBROUTINE THETA
C    NEWTON-RAPHSON OUTER LOOP
      COMMON B,PI,R1,R2,R3,R4,R5,R6,R7,R8,R10,R11,R12,R13,R14,R15,
     1R19,R20,R22,R23,R30,R31,R32,R33,R34,R53,AN1,AN2,FLG2,R73,S
     1,R61,HOLD,KOUNT,ADD,R123,R26,RET,ANG,HTF,R0,EOH,R34R,ACC,CTAVG
      REAL LA(10),LB(10),LC(10),LOH,M,N,NUM,NO,NF
      KOUNT=KOUNT+1 $ IF(KOUNT.GT.15)HOLD=1. $ ADD=0.
      IF(HOLD.EQ.1.)RETURN
      CALL PHI $ IF(FLG2.EQ.1.)GO TO 20 $ IF(HOLD.EQ.1.)RETURN
      R71=R20 $ R62=R8=(R8+R20)/2.
```

```
      CALL PHI $ IF(FLG2.EQ.1.)GO TO 20 $ IF(HOLD.EQ.1.)RETURN
      R72=R20
   15 R100=(R72-R71)/(R62-R61) $ R63=R8=(R71-R100*R61)/(1.-R100)
      CONS=1.
   26 CALL PHI $ IF(FLG2.EQ.1.)GO TO 20 $ IF(HOLD.EQ.1.)RETURN $ R73=R20
      IF(ABS(R62-R72).GT.ABS(R63-R73))GO TO 31 $ IF(CONS.GT.10.)GO TO 31
      R63=R8=R0*R63+(1.-R0)*R62 $ CONS=CONS+1. $ GO TO 26
   31 R61=R62 $ R62=R63 $ R71=R72 $ R72=R73 $ GO TO 15
   20 R15=(R4+R5)/(2.*R5)+(R5-R4)/(2.*R5)*(SIN(2.*R14)-SIN(2.*R8))/(2.*
     1(R14-R8)) $ FLG2=0.
      EOH=SIN(R19)*SIN(R19)*(COS(R14)*COS(R14)/R4+SIN(R14)*SIN(R14)/R5)
     1+COS(R19)*COS(R19)/R6
      R=SQRT(R6*(R4*EOH-1.)/(R4-R6)) $ Q=SQRT(R5*(1.-R6*EOH)/(R5-R6))
      P=SQRT(R4*(1.-R6*EOH)/(R4-R6))
      LOH=SQRT((R5-R6)*(R4*EOH-1.)/(R4*R5*R6))
      M=(R4-R5)*(1.-R6*EOH)/(R5-R6)/(R4*EOH-1.) $ SWITCH=0.
      LA(1)=1. $ LB(1)=SQRT(1.-M) $ LC(1)=SQRT(M) $ N=1. $ I=2
   25 LA(I)=(LA(I-1)+LB(I-1))/2. $ LB(I)=SQRT(LA(I-1)*LB(I-1))
      LC(I)=(LA(I-1)-LB(I-1))/2. $ N=N+1.
      IF(LC(I).LT.1.E-6)GO TO 30 $ I=I+1 $ GO TO 25
   30 NO=SIN(R8)/Q $ DO=COS(R8)/P $ NF=SIN(R14)/Q $ DF=COS(R14)/P
      R8I=AINT(2.*R8/PI) $ R14I=AINT(2.*R14/PI)
      UO=ATAN2(NO,DO) $ UOI=AINT(2.*UO/PI)
      IF(R8I.EQ.UOI)GO TO 52 $ UO=UO+PI/2.*(R8I-UOI)
      IF(AMOD(R8I,4.).NE.AMOD(UOI,4.))UO=UO+ABS(R8-UO)/(R8-UO)*PI/2.
   52 NUM=1. $ I=1 $ PBN=UO
   35 QN=AINT(2.*PBN/PI)+ABS(PBN)/PBN
      QUAD=QN-ABS(PBN)/PBN $ IF(QN/2..EQ.AINT(QN/2.))QUAD=QN
      PB=ATAN(LB(I)*TAN(PBN)/LA(I))+PBN+QUAD*PI/2. $ NUM=NUM+1.
      I=I+1 $ IF(NUM.EQ.N)GO TO 40 $ PBN=PB $ GO TO 35
   40 IF(SWITCH.EQ.1.)GO TO 45 $ SWITCH=1. $ EPS=PB/(2.**(N-1.)*LA(I))
      I=1 $ UF=ATAN2(NF,DF) $ UFI=AINT(2.*UF/PI)
      IF(R14I.EQ.UFI)GO TO 53 $ UF=UF+PI/2.*(R14I-UFI)
      IF(AMOD(R14I,4.).NE.AMOD(UFI,4.))UF=UF+ABS(R14-UF)/(R14-UF)*PI/2.
   53 NUM=1. $ PBN=UF $ GO TO 35
   45 HTF=(PB/(2.**(N-1.)*LA(I))-EPS)/LOH*ABS(R4-R6)/(R4-R6)
      CTAVG=ABS(R*(UF-UO)/(LOH*HTF))
      R34=HTF*R15/R4 $ R34R=R34-2.*PI*INT(R34/(2.*PI))
    5 R53=R30=R7*ABS(R13/R34R)**.1
      IF(ABS(R34R).GT.PI)R53=R30=R7*ABS(R13/(2.*PI-ABS(R34R)))**.1
      IF(R30.LE.R2/6.0)HOLD=1.
      RETURN $ END


      SUBROUTINE PHI
C     NEWTON-RAPHSON INNER LOOP
```

```
   COMMON B,PI,R1,R2,R3,R4,R5,R6,R7,R8,R10,R11,R12,R13,R14,R15,
  1R19,R20,R22,R23,R30,R31,R32,R33,R34,R53,AN1,AN2,FLG2,R73,S
  1,R61,HOLD,KOUNT,ADD,R123,R26,RET,ANG,HTF,RO,EOH,R34R,ACC,CTAVG
   ADD=ADD+1. $ IF(ADD.LT.20.)GO TO 10
   HOLD=1. $ RETURN
10 R9=(R5*(R6-R4)*COS(R8)*COS(R8)+R4*(R6-R5)*SIN(R8)*SIN(R8))*SIN(R7)
  1*SIN(R7)
   R10=R9/(R6*(R4-R5)*SIN(R7)*SIN(R7)*COS(R8)*COS(R8)+R4*(R6-R5)*
  1COS(R7)*COS(R7)) $ IF(R10.GE.0.)GO TO 20
   R47=ATAN(SQRT(R4*(R6-R5)/(ABS(R6-R5)/(R6-R5)+R6*(R5-R4)*COS(R8)
  1*COS(R8)))) $ RAN=ABS(R7*R8)/200.
15 IF(RAN.LE..05)GO TO 16
   RAN=RAN/2. $ GO TO 15
16 R47=R47*(1.-RAN)
   IF(R7.EQ.R31)R31=R47 $ IF(R7.EQ.R32)R32=R47
   IF(R7.EQ.R33)R33=R47 $ R7=R47 $ GO TO 10
20 R10=ATAN(SQRT(R10))
   AN1=PI-R1-R8
   R11=ATAN(SIN(.5*(R2-R7))/(SIN(.5*(R2+R7))*TAN(.5*AN1)))
   R12=ATAN(COS(.5*(R2-R7))/(COS(.5*(R2+R7))*TAN(.5*AN1)))
   R13=R11+R12 $ PATH=1.-2.*R123
   IF(0..GT.R13*PATH*(2.*B-1.))R13=R13-PI*ABS(R13)/R13
   R14=R13-2.*R11+R3
5  IF(0..LT.R13*PATH*(R14-R8)*(R4-R6))GO TO 9
   R14=R14+2.*PI*PATH
   IF((R14-R8)*PATH.GT.2.*PI)R14=R14-4.*PI*PATH $ GO TO 5
 9 R18=R5*(R6-R4)*COS(R14)*COS(R14)+R4*(R6-R5)*SIN(R14)*SIN(R14)-R6
  1*(R4-R5)*COS(R14)*COS(R14)*TAN(R10)*TAN(R10)
   R19=ATAN(SQRT(R4*(R6-R5)*TAN(R10)*TAN(R10)/R18))
   S=.5*(R7+R19+R2)
   IF((S-R2)*(S-R7)*(S-R19).GT.0.)GO TO 8 $ HOLD=1. $ RETURN
 8 R46=SIN(S-R7)*SIN(S-R2)*SIN(S-R19)/SIN(S)
   R23=ABS(2.*ATAN(SQRT(R46)/SIN(S-R19)))*ABS(R13)/R13
   R20=PI-R1-R23
   FLG2=0. $ IF(ABS((R8-R20)/R8).LE.ACC)FLG2=1.
 4 FORMAT(6X8E14.4)
   RETURN $ END


   SUBROUTINE EULER(N,T,Y,DYDT)
   COMMON /EULER/C4,C5,C6,H
   DIMENSION Y(3),DYDT(3)
   DYDT(1)=H*(SIN(Y(3))*SIN(Y(3))/C5+COS(Y(3))*COS(Y(3))/C4)
   DYDT(2)=H*(1./C5-1./C4)*SIN(Y(2))*SIN(Y(3))*COS(Y(3))
   DYDT(3)=COS(Y(2))*(H/C6-DYDT(1))
   RETURN $ END
```

APPENDIX B

POLHODE AXES

Poinsot's geometric solution, described in reference 8, equates the free rotational motion of a rigid body to the motion of the "ellipsoid of inertia" for that body as it rolls on the "invariable plane." The point of intersection between these two surfaces traces out a "polhode" curve on the ellipsoid of inertia. The axis surrounded by the polhode curve, or "polhode axis," is the principal body axis which precesses about the momentum vector during a coning maneuver. The polhode axis, which can be an axis of minimum moment of inertia or an axis of maximum moment of inertia but not an axis of intermediate moment of inertia, is related to the initial motion and the inertial distribution of the body as follows:

$$\left.\begin{array}{l}\text{Polhode is about the x-axis if} \\ \qquad \tan^2\theta\cos^2\phi > \dfrac{I_x(I_y - I_z)}{I_z(I_x - I_y)} \\ \text{Polhode is about the z-axis if} \\ \qquad \tan^2\theta\cos^2\phi < \dfrac{I_x(I_y - I_z)}{I_z(I_x - I_y)}\end{array}\right\} \qquad \text{(B1)}$$

where θ and ϕ are evaluated simultaneously at any time during the maneuver. Conditions (B1) can be determined directly from equations (11) and the requirement that θ_{max} be real-valued.

It should be mentioned that the derivation of equation (11a) was based upon θ being measured from the polhode axis. This condition is met in the present paper for motions with polhodes about the z-axis, but not for polhodes about the x-axis. Rather than rederive the motion equations with θ measured from the x-axis, the two-step alternative used in reference 4 was used. That is, for polhode about the x-axis, the values of I_x and I_z were interchanged and the original Euler rotations about the z-, y-, and z-axes were replaced with a newly generated set of Euler rotations about the -x-, y-, and -x-axes designed to produce the identical body reorientation. The new Euler set was determined by the method of reference 9 and implemented in program IMP2 of appendix A. With these changes, the coning geometry is transferred, in effect, from polhode about the z-axis to polhode about the x-axis.

APPENDIX C

AVERAGE REORIENTATION COSTS FOR ROD-SHAPED BODIES

The derivation of average reorientation costs for rod-shaped bodies is presented in appendix C of reference 4. Costs for rod-shaped bodies with axial symmetry along the x-axis ($I_x \to 0$; $I_y = I_z$) as well as rod-shaped bodies with axial symmetry along the z-axis ($I_z \to 0$; $I_x = I_y$) are specified by the equation

$$(\text{Average cost}) = \frac{8}{\pi} R_{2,\text{mean}} \tag{C1}$$

However, in application of this equation reference 4 uses incorrect values for $R_{2,\text{mean}}$. Correct values of $R_{2,\text{mean}}$, derived for rod-shaped bodies with axial symmetry along the z-axis, are expressed as a function of maneuver range by

$$R_{2,\text{mean}} = \frac{\sin R_{2,\max} - R_{2,\max} \cos R_{2,\max}}{1 - \cos R_{2,\max}}$$

For rod-shaped bodies with axial symmetry along the x-axis, all coning maneuvers are "polhode about the x-axis" and $R_{2,\text{mean}}$ is determined by averaging R_{2C}, the second angle of the transformed Euler angle set. The average value of R_{2C} was determined numerically to be equal to $\pi/2$ radians for all values of $R_{2,\max}$.

Values of $R_{2,\text{mean}}$ and average cost are listed as follows for pertinent values of $R_{2,\max}$ and for both inertial configurations:

	Selected values of $R_{2,\max}$, radians				
	0.00873	$\pi/4$	$\pi/2$	$3\pi/4$	π
Rod-shaped with axial symmetry about x-axis					
$R_{2,\text{mean}}$	$\pi/2$	$\pi/2$	$\pi/2$	$\pi/2$	$\pi/2$
Average cost . .	4	4	4	4	4
Rod-shaped with axial symmetry about z-axis					
$R_{2,\text{mean}}$	0.00582	0.5181	1.00	1.390	$\pi/2$
Average cost . .	0.01481	1.319	2.547	3.540	4

These values of average cost are presented in figure 6.

REFERENCES

1. Grubin, Carl: Generalized Two-Impulse Scheme for Reorienting a Spin Stabilized Vehicle. Guidance and Control, Robert E. Roberson and James S. Farrior, eds., Academic Press, 1962, pp. 649-668.

2. Grubin, Carl: Two-Impulse Attitude Reorientation of an Asymmetric Spinning Vehicle. AIAA Symposium on Structural Dynamics and Aeroelasticity, Aug.-Sept. 1965, pp. 245-249.

3. Dixon, M. V.; Edelbaum, T. N.; Potter, J. E.; Vandervelde, W. F.: Fuel Optimal Reorientation of Axisymmetric Spacecraft. Rep. No. SAMSO-TR-70-184, U.S. Air Force, Mar. 15, 1970. (Available from DDC as AD 706 386.)

4. Martz, C. William: Attitude Reorientation of Spacecraft by Means of Impulse Coning. NASA TN D-8452, 1977.

5. Selby, Samuel M., ed.: Standard Mathematical Tables. Eighteenth ed. Chem. Rubber Co., c.1970.

6. Whittaker, E. T.: A Treatise on the Analytical Dynamics of Particles and Rigid Bodies. Fourth ed. Cambridge Univ. Press, 1964.

7. Abramowitz, Milton; and Stegun, Irene A., eds.: Handbook of Mathematical Functions with Formulas, Graphs, and Mathematical Tables. NBS Appl. Math. Ser. 55, U. S. Dep. Commer., June 1964.

8. Greenwood, Donald T.: Principles of Dynamics. Prentice-Hall, Inc., c.1965.

9. Meyer, George; Lee, Homer Q.; and Wehrend, William R., Jr.: A Method for Expanding a Direction Cosine Matrix Into an Euler Sequence of Rotations. NASA TM X-1384, 1967.

TABLE I.- COST STATISTICS FOR $I_y = 100$

I_x	I_z	Cost at selected values of $R_{2,max}$, radians, of -									
		$\pi/360$		$\pi/4$		$\pi/2$		$3\pi/4$		π	
		Av. cost	SDA	Av. cost	SDA	Av. cost	SDA	Av. cost	SDA	Av. cost	SDA
199	99			4.79	0.60	5.57	0.47	5.91	0.39	6.05	0.37
195	95	5.01	0.74								
180	80	3.72	.71	4.87	.51	5.88	.51	5.93	.45	6.02	.43
160	99			5.16	.64	5.73	.48	6.14	.40	6.28	.37
160	95	4.60	.75								
160	80	3.54	.68	4.83	.51	5.85	.50	6.00	.45	6.08	.42
160	60	3.10	.65	4.28	.48	5.59	.48	6.13	.47	6.16	.46
140	40	1.68	.57	3.16	.38	4.65	.39	5.82	.45	5.86	.45
120	99	4.20	.86	5.50	.72	6.26	.54	6.68	.45	6.80	.42
120	95	4.36	.71								
120	80	3.12	.60	4.60	.50	5.72	.46	6.34	.44	6.48	.43
120	60	3.04	.67	4.42	.54	5.53	.46	6.27	.43	6.34	.42
120	40	1.71	.58	3.12	.39	4.58	.38	5.73	.42	5.87	.42
120	20	.83	.61	2.14	.34	3.53	.36	4.59	.39	4.98	.42
110	10	.43	.65	1.73	.34	3.05	.36	4.07	.39	4.50	.42
100+	95	4.00	.76								
100+	80	2.84	.55	4.69	.56	5.67	.41	6.53	.37	6.79	.36
100+	60	2.81	.68	4.36	.48	5.54	.43	6.25	.36	6.48	.34
100+	40	1.8	.60	3.32	.42	4.67	.38	5.68	.37	5.97	.36
100+	20	.84	.62	2.09	.34	3.33	.33	4.32	.36	4.79	.39
100+	10	.41	.64	1.65	.32	2.90	.35	3.88	.38	4.33	.41
100-	200-	2.73	.58	4.46	.50	5.61	.42	6.26	.35	6.53	.34
100-	180	2.73	.57	4.43	.50	5.64	.43	6.42	.37	6.65	.35
100-	160	2.88	.69	4.52	.51	5.70	.43	6.46	.37	6.76	.36
100-	140	2.74	.55	4.64	.54	5.70	.43	6.54	.37	6.78	.36
100-	120	2.94	.57	4.87	.60	6.09	.47	7.35	.43	7.50	.41
80	180	2.48	.63	3.78	.51	4.94	.41	5.95	.42	6.20	.43
80	160	2.62	.72	3.94	.58	5.05	.44	6.01	.43	6.25	.43
80	140	2.51	.62	3.88	.52	5.12	.44	6.04	.43	6.26	.42
80	120	2.58	.61	4.18	.59	5.41	.49	6.14	.43	6.30	.41
80	110	2.91	.77	4.47	.69	5.72	.52	6.23	.43	6.40	.41
80	101			5.12	.69	5.93	.51	6.40	.42	6.55	.39
60	160	2.23	.74	3.45	.57	5.21	.55	5.86	.47	5.98	.44
40	140	1.97	.89	3.39	.64	5.32	.55	5.58	.47	5.66	.45
40	120			4.04	.68	5.44	.53	5.62	.46	5.68	.44
40	101			4.94	.59	5.46	.48	5.54	.42	5.61	.41
20	120			4.38	.63	4.90	.48	4.96	.44	5.01	.43
10	110			4.55	.52	4.55	.43	4.54	.41	4.55	.42

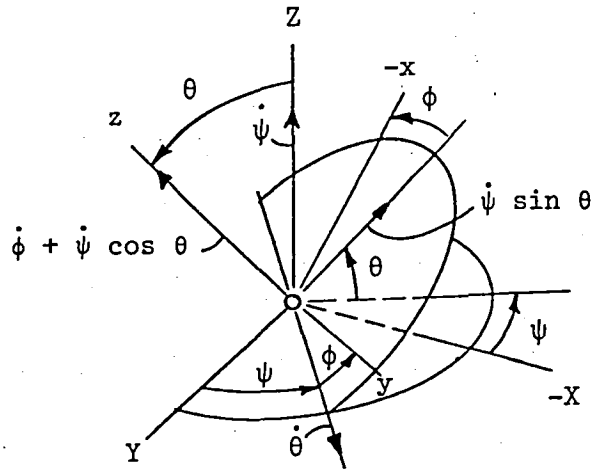

(a) Inertial rate components.

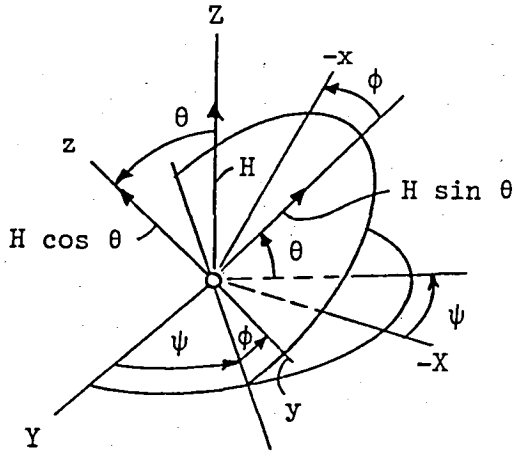

(b) Angular momentum components.

Figure 1.- Orientation of body and inertial coordinate axes systems for Euler rotation sequence ψ,θ,ϕ about body axes z,y,z, respectively.

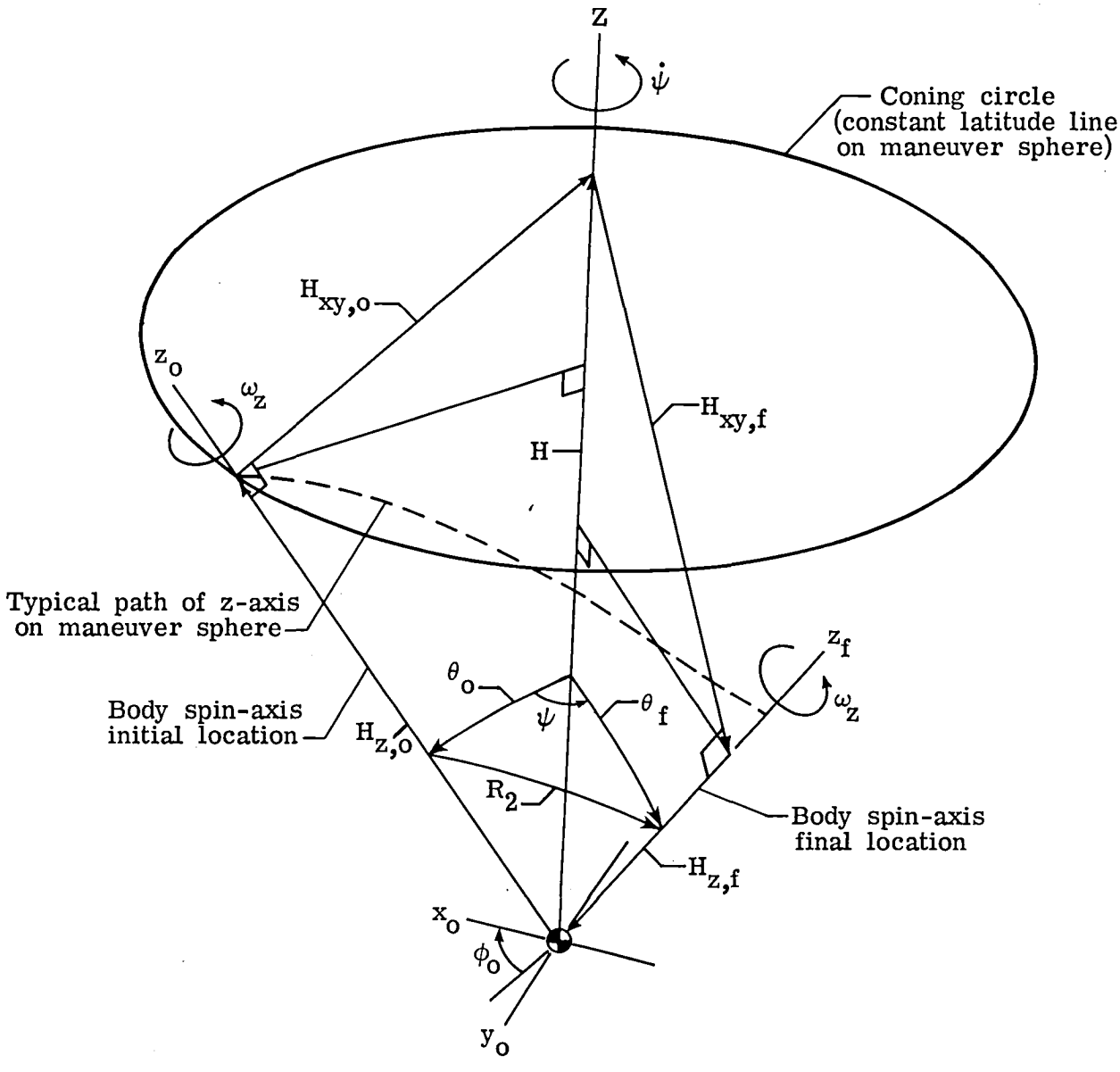

Figure 2.- Coning geometry showing momentum components.

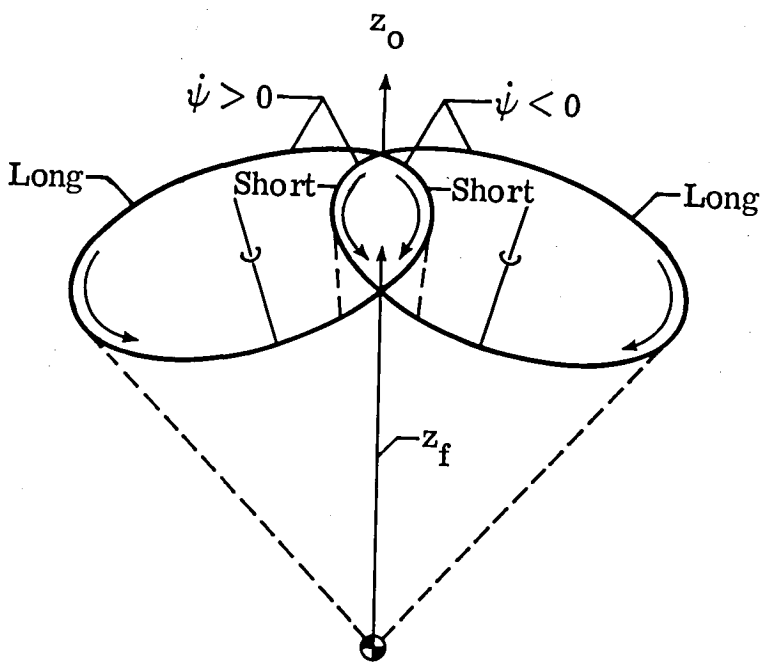

Figure 3.- Basic coning-path options (short and long paths for both positive and negative coning rates). Nutational motions are suppressed for clarity.

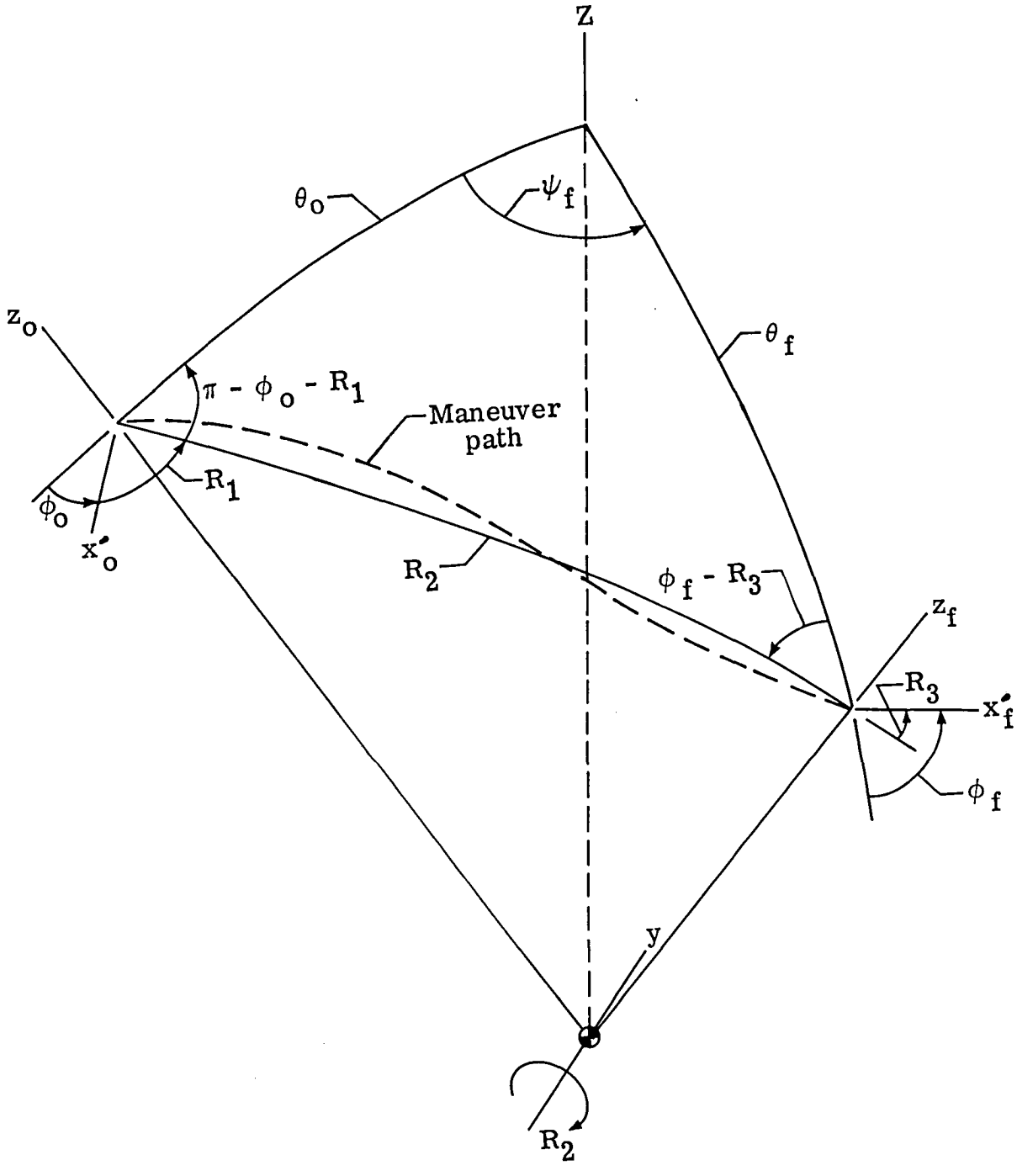

Figure 4.- Geometry of generalized maneuver R_1, R_2, and R_3 illustrating the spherical-triangle and spin-angle relationships. Positive angles are measured clockwise about axis of rotation.

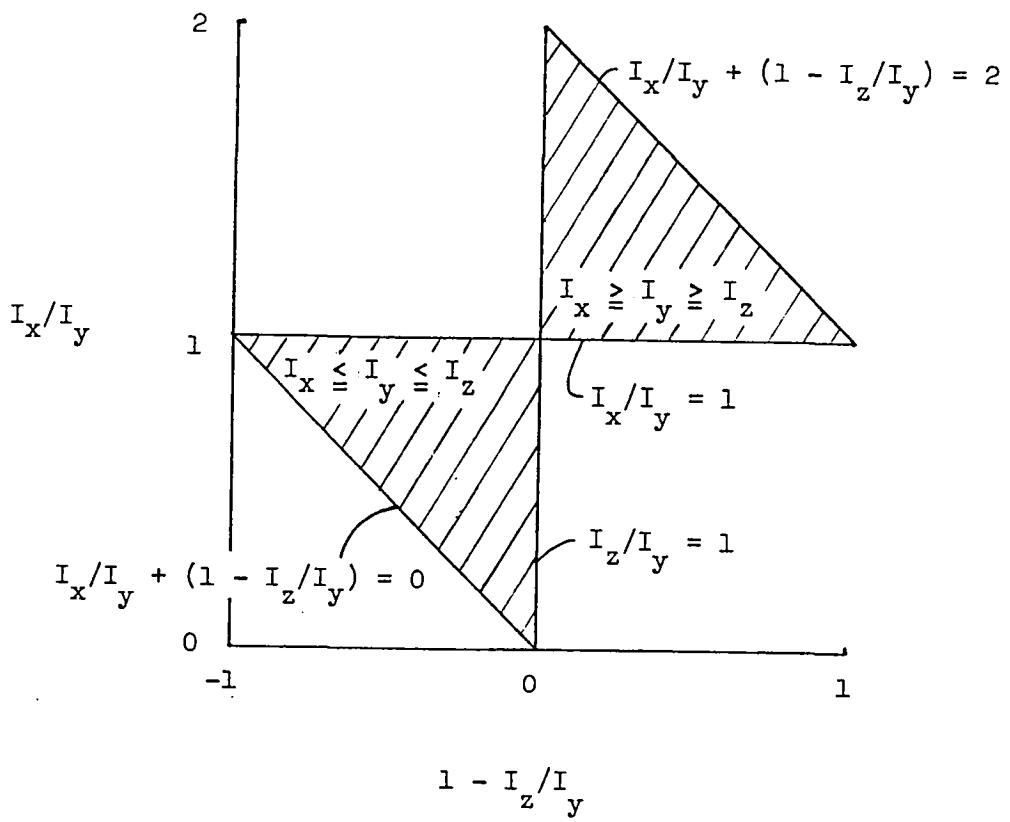

Figure 5.- Inertia constraints. All real bodies are in shaded areas.

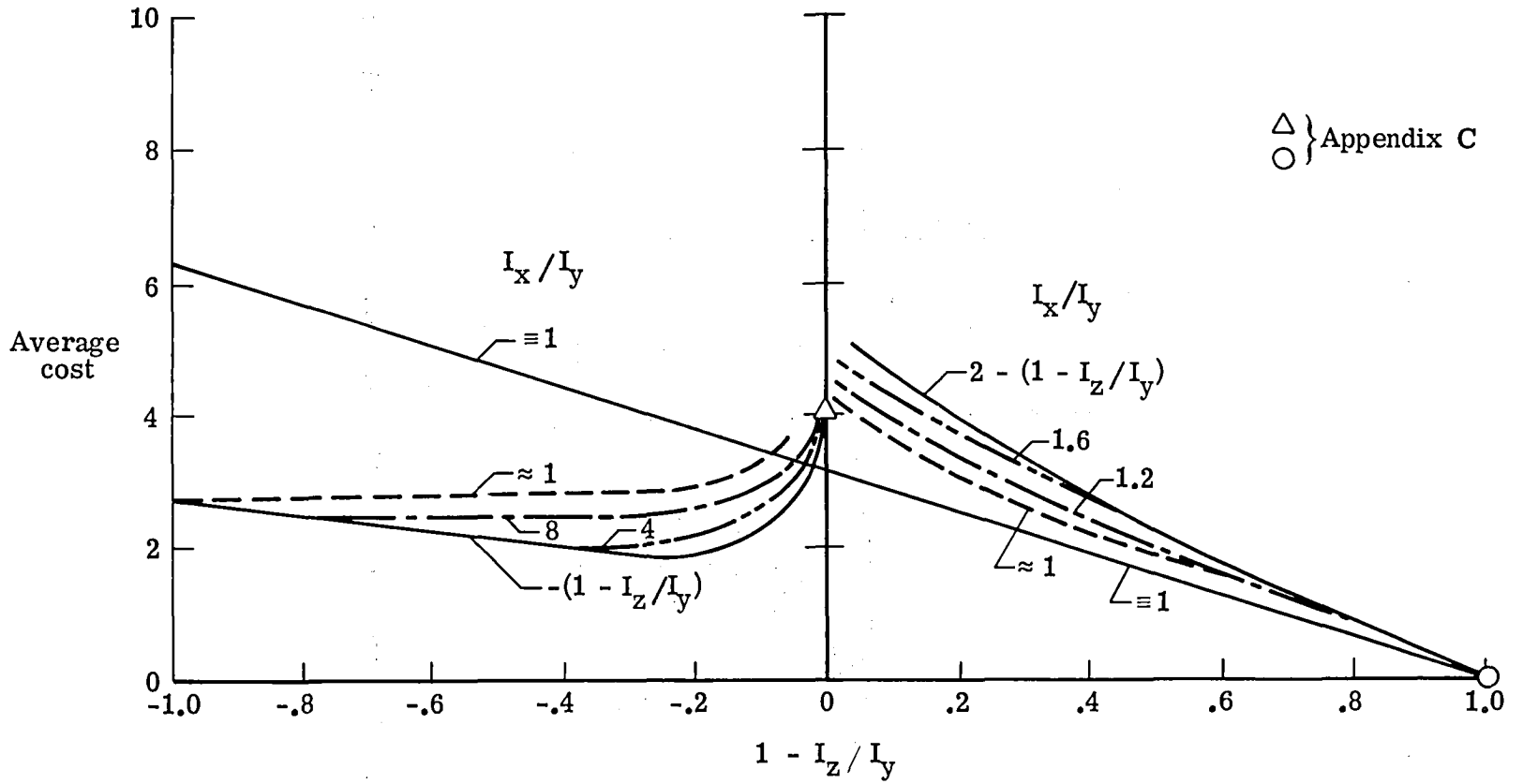

(a) Maneuver range, π/360 radians.

Figure 6.- Effect of inertia distribution on average cost of reorientation.

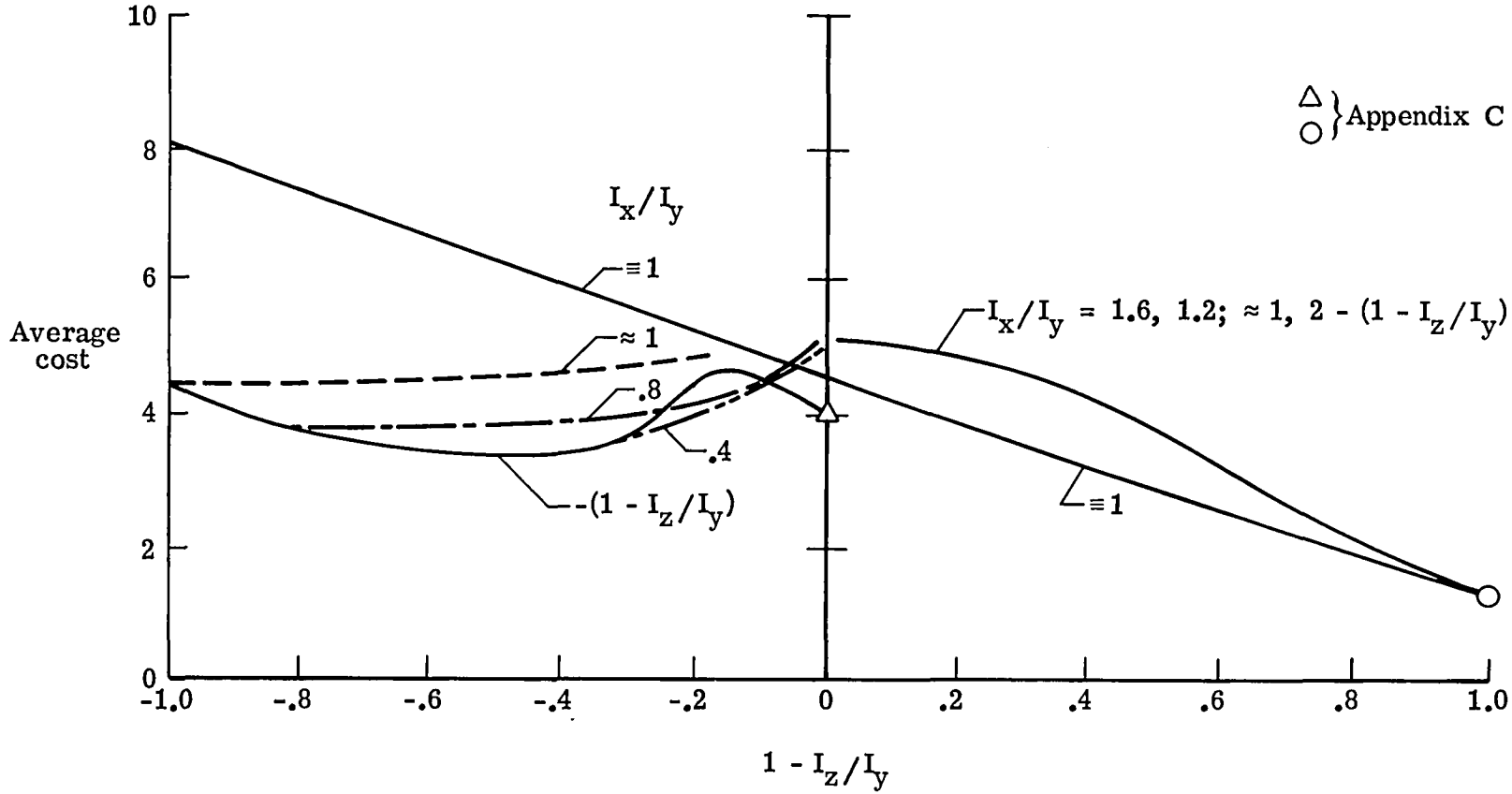

(b) Maneuver range, $\pi/4$ radians.

Figure 6.- Continued.

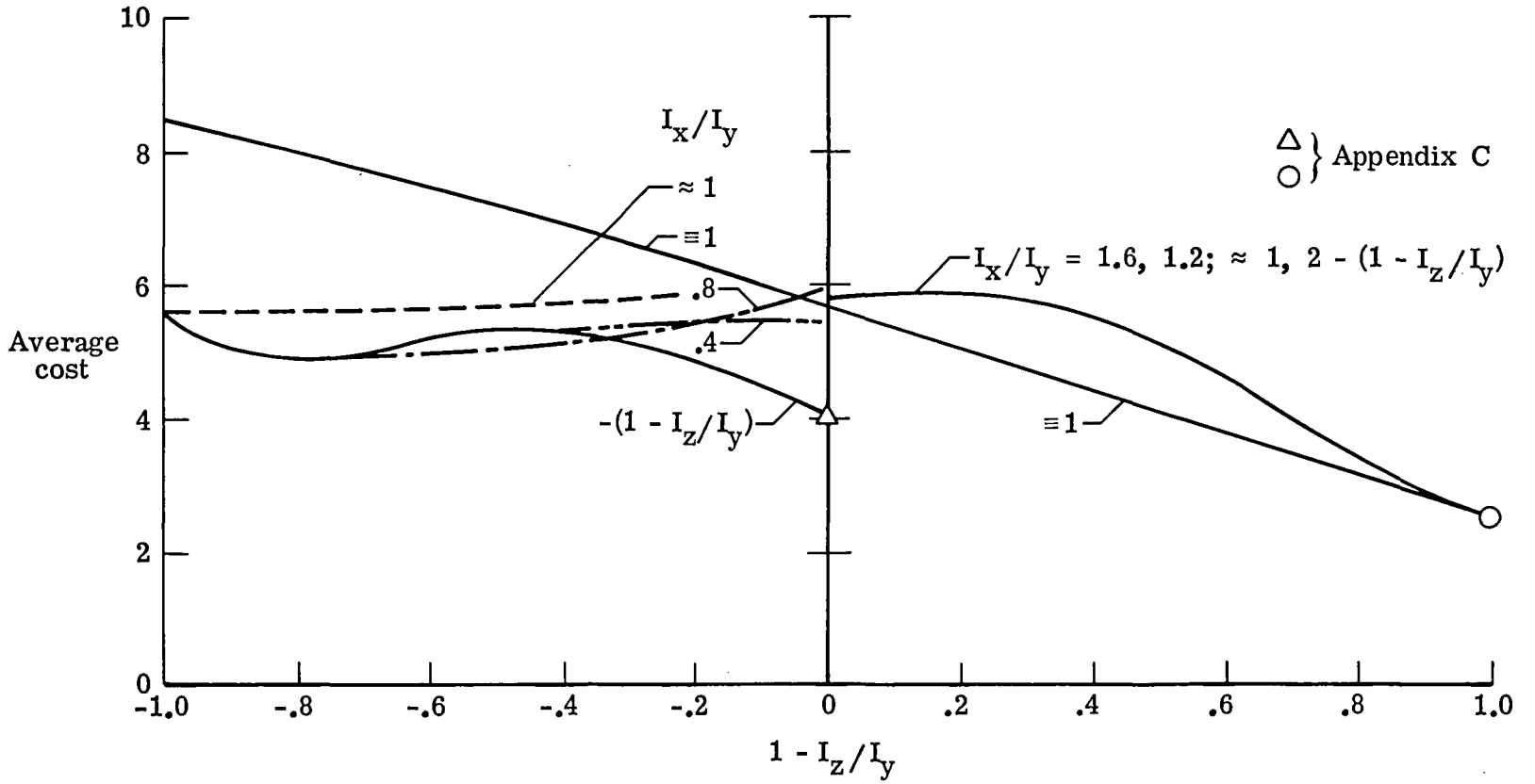

(c) Maneuver range, $\pi/2$ radians.

Figure 6.- Continued.

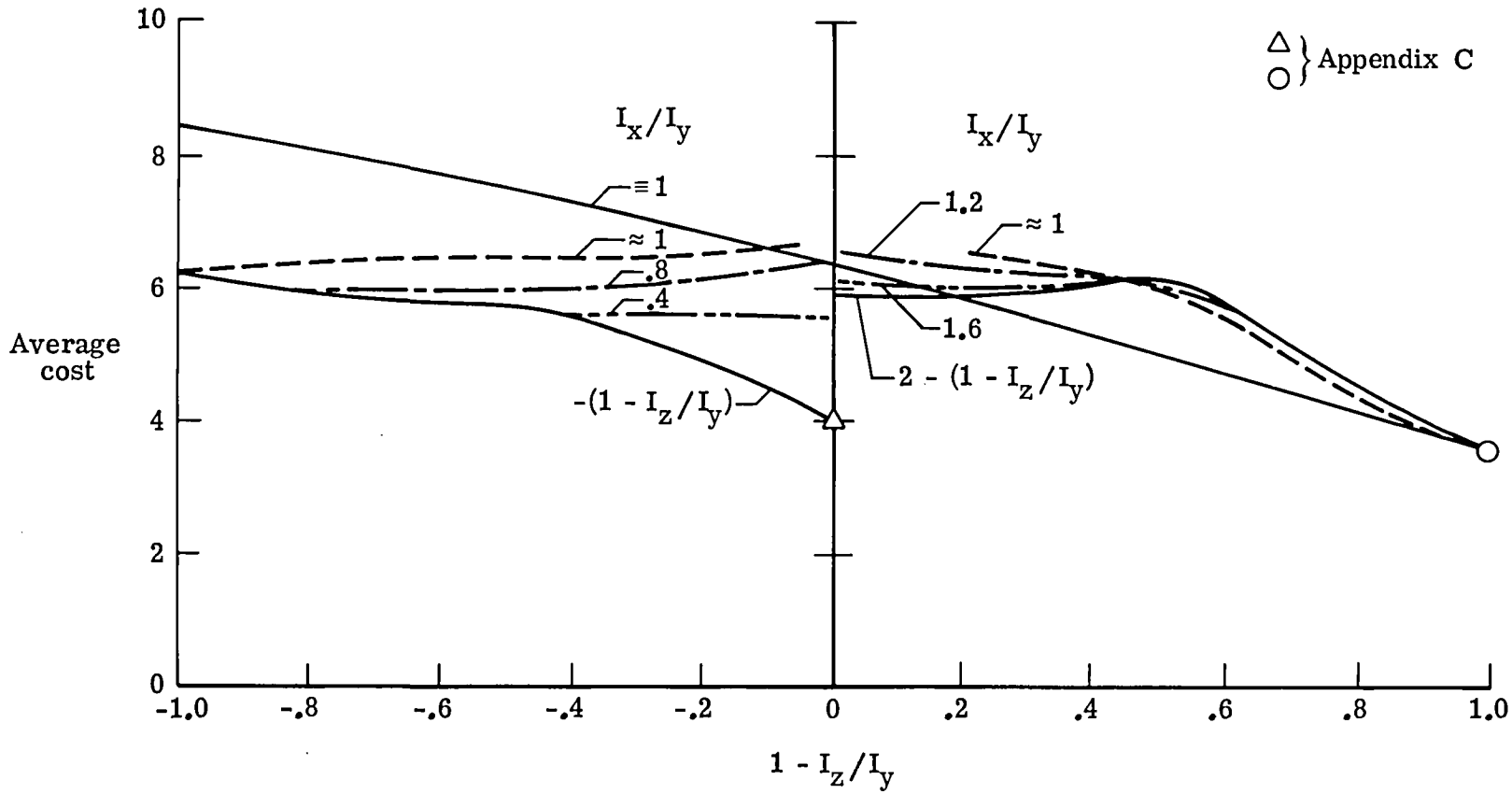

(d) Maneuver range, $3\pi/4$ radians.

Figure 6.- Continued.

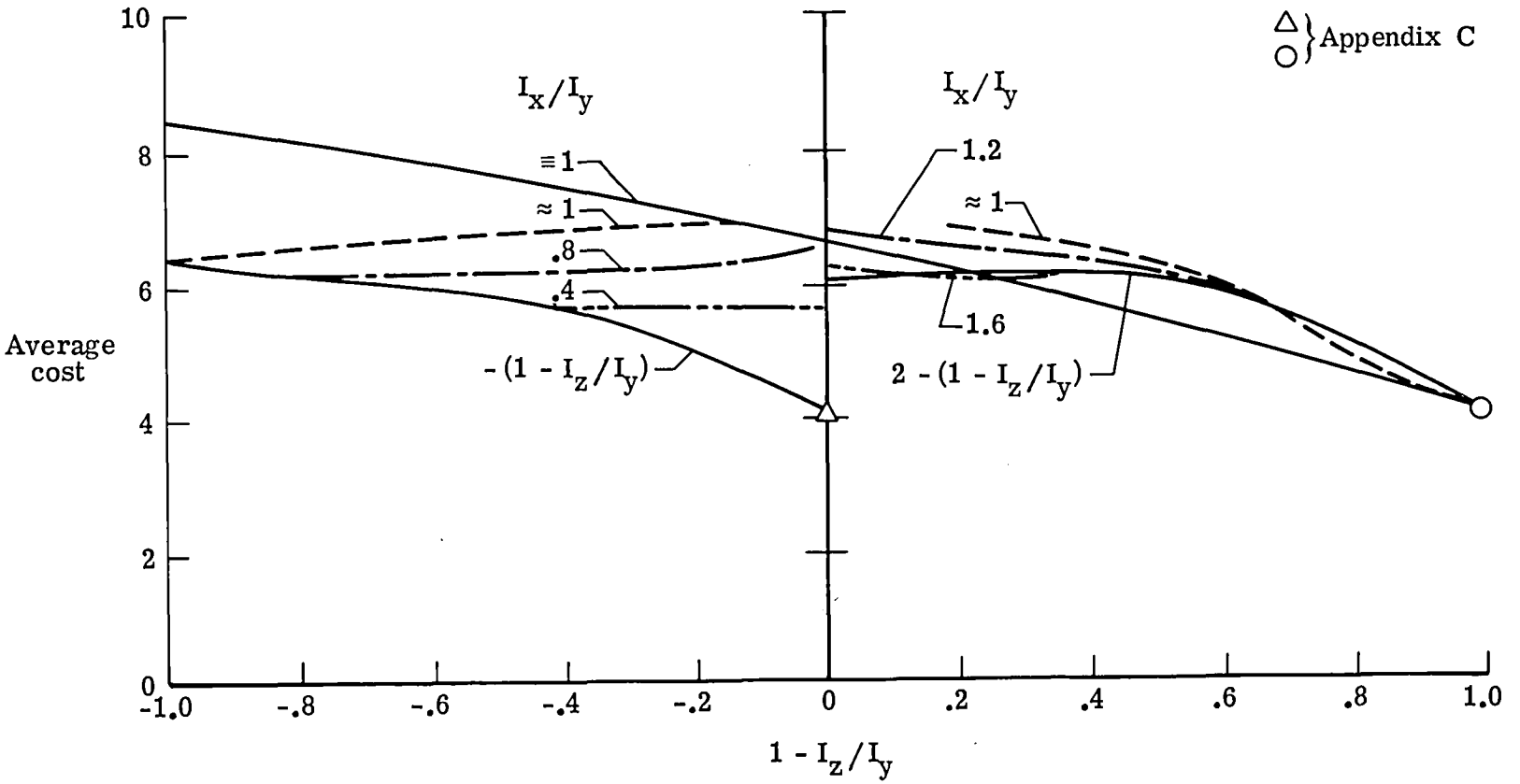

(e) Maneuver range, π radians (all possible reorientations).

Figure 6.- Concluded.

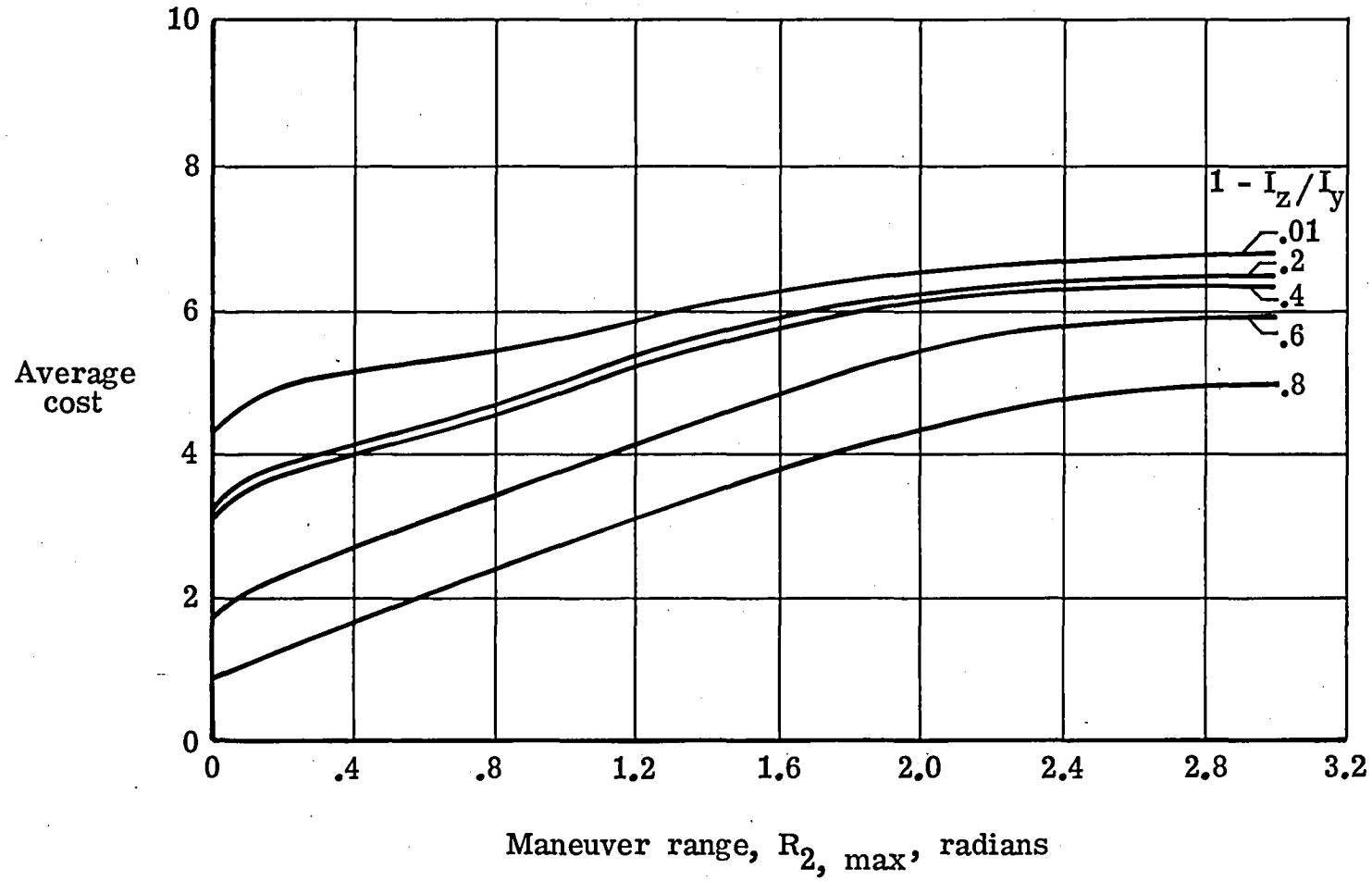

Figure 7.- Effect of maneuver range on average cost of reorientation for asymmetric bodies with $I_x/I_y = 1.2$.

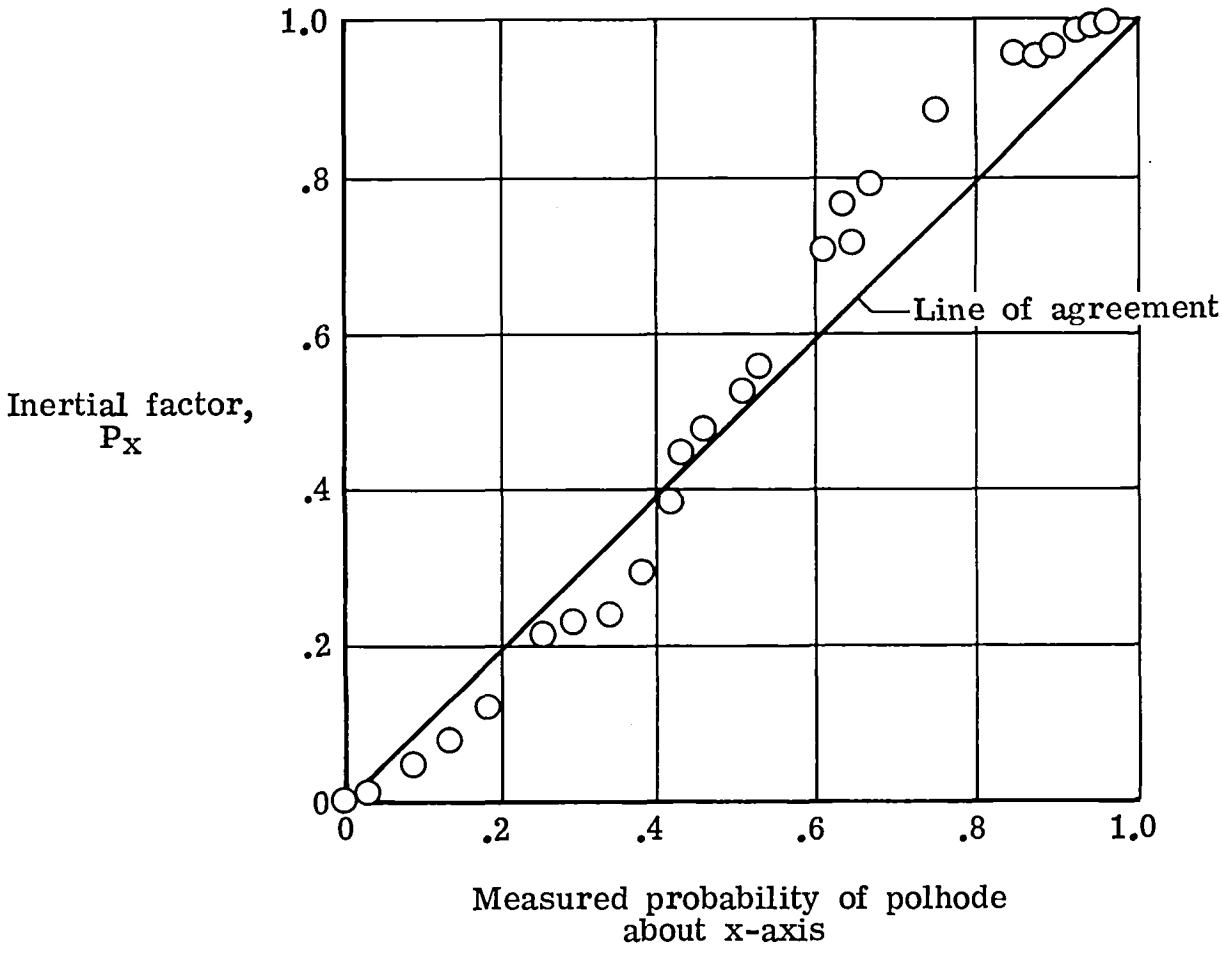

Figure 8.- Correlation of inertial factor P_x with measured probability of polhode about x-axis. $R_{2,max} = \pi$ radians.

1. Report No.	2. Government Accession No.	3. Recipient's Catalog No.
NASA TP-1554		

4. Title and Subtitle	5. Report Date
TWO-IMPULSE REORIENTATION OF ASYMMETRIC SPACECRAFT	December 1979
	6. Performing Organization Code

7. Author(s)	8. Performing Organization Report No.
C. William Martz	L-12921
	10. Work Unit No. 506-54-23-01

9. Performing Organization Name and Address	11. Contract or Grant No.
NASA Langley Research Center Hampton, VA 23665	
	13. Type of Report and Period Covered: Technical Paper

12. Sponsoring Agency Name and Address	14. Sponsoring Agency Code
National Aeronautics and Space Administration Washington, DC 20546	

15. Supplementary Notes

16. Abstract

An investigation has been conducted to determine minimum "maneuver costs" for attitude reorientation of spacecraft of all possible inertial distribution over a wide range of maneuver angles by use of a two-impulse coning method of reorientation. Maneuver cost is proportional to the product of fuel consumed (total impulse) and time expended during a maneuver. Assumptions included external impulsive control torques, rigid-body spacecraft rest-to-rest maneuvers, and no disturbance torques. Results are presented in terms of average cost and standard deviation for various maneuver ranges. Costs of individual reorientations can be calculated with the computer program included.

17. Key Words (Suggested by Author(s))	18. Distribution Statement
Spacecraft attitude control Spacecraft maneuvering Attitude reorientation Impulse coning Inertia constraints	Unclassified - Unlimited Subject Category 13

19. Security Classif. (of this report)	20. Security Classif. (of this page)	21. No. of Pages	22. Price*
Unclassified	Unclassified	40	$4.50

* For sale by the National Technical Information Service, Springfield, Virginia 22161

National Aeronautics and Space Administration

Washington, D.C.
20546

Official Business
Penalty for Private Use, $300

THIRD-CLASS BULK RATE

Postage and Fees Paid
National Aeronautics and
Space Administration
NASA-451

NASA

POSTMASTER: If Undeliverable (Section 158 Postal Manual) Do Not Return